1-1-2003

The effects of slope and flexural deflection on the concrete-dowel bar system

Andrew Lewis Lundy
Iowa State University

The effects of slope and flexural deflection on the concrete-dowel bar system

by

Andrew Lewis Lundy

A thesis submitted to the graduate faculty

in partial fulfillment of the requirements for the degree of

MASTER OF SCIENCE

Major: Civil Engineering (Structural Engineering)

Program of Study Committee:
Max L. Porter, Major Professor
James K. Cable
Lester W. Schmerr Jr.

Iowa State University

Ames, Iowa

2003

Graduate College

Iowa State University

This is to certify that the Master's thesis of

Andrew Lewis Lundy

has met the thesis requirements of Iowa State University

Signatures have been redacted for privacy

TABLE OF CONTENTS

LIST OF FIGURES

LIST OF TABLES

ABSTRACT

This paper provides a review of recently completed dowel bar research at Iowa State University. This paper also looks at the assumptions used in this research and checks these against the theoretical analysis of these assumptions.

The assumptions that are reviewed are the neglecting of slope deflection and flexural deflection. These terms are theoretically analyzed, evaluated, and then reviewed to check the effects. The effect of each type of deflection was compared against the modulus of dowel support, concrete bearing stress, and influence on conclusions drawn in previous research. This analysis was done to all types of dowel bars for the two most recently completed research projects.

Furthermore, the differences between Timoshenko's dowel bar theory and Friberg's dowel bar theory are analyzed. These theory differences are also outlined for each type of dowel bar.

1.0 INTRODUCTION

1.1 Background

According to the Federal Highway Administration (FHWA) there are approximately 160,000 centerline miles of National Highway System in the United States (1). Of these 160,000 centerline miles, there are 3,180 centerline miles of National Highway System in Iowa (1). 2,860 centerline miles of the 3,180 centerline miles reported were described as a High-Type Rigid Pavement (2). According to the FHWA a High-Type Rigid pavement is defined as: "a Portland cement concrete roadway with or without a bituminous wearing surface of less than 1 in."(2).

In the 2002 Condition and Performance Report to Congress the FHWA reports that 86.6% of the Total System Pavement and 93.5% of the National Highway System Pavement are acceptable (3). Thus, 13.4% and 6.5% of the respective pavements are in unacceptable condition. The unacceptable amount of highway in Iowa is approximately equal to 206 centerline miles. Unfortunately, the FHWA does not differentiate the condition of each type of pavements. Therefore, assuming the same percentage of unacceptable roads for each type of pavement would mean that approximately 185 centerline miles of rigid concrete pavement would be in unacceptable condition.

According to the current Iowa Department of Transportation Standards, there is one doweled contraction joint required every 20 feet for concrete pavements thicker than 8 in. (4). One doweled joint every 20 feet is equivalent to 264 doweled joints per mile. The FHWA's 185 centerline miles of unacceptable pavement should contain over 48,000 doweled joints. While failure of the dowel bars is not the only cause for the unacceptable roads; dowel bars certainly play a large role in the overall condition of the roads.

Load transfer within a series of concrete slabs takes place across the joints. For a typical concrete paved road, these joints are approximately 1/8-in. gaps between two adjacent slabs. Dowel bars are located at these joints and are used to transfer load from one slab to the adjacent slab. As long as the dowel bar is completely surrounded by concrete no problems will occur. However, when the hole starts to oblong, a void space is created and difficulties can arise. This void space is formed due to a stress concentration where the dowel contacts the concrete. Over time, the repeated process of traffic traveling over the joint crushes the concrete surrounding the dowel bar and causes a void in the concrete. This void inhibits the dowel bar's ability to effectively transfer load across the joint. Furthermore, this void gives water and other particles a place to collect that will eventually corrode and potentially bind or lock the joint so that no thermal expansion is allowed. Once there is no longer load transferred across the joint, the load is transferred to the subgrade and faulting or pumping can occur. Faulting is defined as the difference between adjacent slabs, which is caused by differential settlement. Faulting at the joint creates a roughness, making vehicle travel uncomfortable, and requires that the slab be repaired or replaced. Pumping is the expulsion of subgrade material through joints and along the edges of the pavement. Pumping accelerates the deterioration of the joint since subgrade support for the slab is diminished.

As was mentioned in the previous paragraph, a void around a dowel bar is formed by stress concentrations crushing the concrete directly in contact with the dowel. When a shear load is applied to the concrete slab, the force is supported only by the top or bottom of the dowel bar, not the sides. Since the stress concentration region lies on the top or bottom of the dowel bar, the smaller the dowel bar the higher the stress concentration for the same load. The sides of the dowel bars do not aid in the distribution of the shear load from the concrete.

Therefore, the top and bottom of the dowel bar is where the stress concentration is located and is directly related to the width, shape and/or material of the dowel bar.

1.2 Objective

Previous work done at Iowa State University (ISU) by Guinn outlined areas where gaps existed on previous research done around the nation (5). Guinn outlined twenty-two areas where gaps were present in dowel bar research. Using the information from Guinn the following objectives were set for this paper:

- to discuss the types of analysis used in previous research at ISU,
- to discuss the assumptions made in previous dowel bar research completed at ISU,
- to evaluate the appropriateness of the assumptions used in previous research, and
- to recommend any changes that should be implemented with future research programs.

1.3 Scope

The scope of this paper was as follows:

- summarize the recently completed research done at ISU,
- highlight the differences between the Timoshenko and Friberg theories,
- determination of the effects of slope deflection on the modulus of dowel support and bearing stress,
- determination of the effects of flexural deflection on the modulus of dowel support and bearing stress,
- determination of the effects of slope deflection and flexural deflection on previous research, and

- determination of when to consider the effects of slope deflection and flexural deflection.

2.0 Literature Review

2.1 Introduction

ISU has been conducting dowel bar research for over ten years. Throughout these years, two primary theoretical models have been utilized. One common model is based on work done by Timoshenko and Lessels. Timoshenko's principles were based on a beam resting on an elastic foundation. Later, Friberg expanded on Timoshenko's work and came up with a second model that could be used for dowel bar research.

2.2 Analytical Theory of Dowel Bars

2.2.1 Analytical Model

2.2.1.1 Timoshenko's Analytical Model

Timoshenko and Lessels worked on the first model of a beam on an elastic foundation that could be applied to a dowel bar system (6). According to Timoshenko, the deflection of a beam on an elastic foundation is found using Equation 2.1:

$$EI\frac{d^4y}{dx^4} = -ky \qquad (2.1)$$

where k is a constant, usually called the modulus of foundation (psi), E is the modulus of elasticity of the beam (psi), I is the moment of inertia of the beam ($in.^4$), and y is the deflection (in.). The modulus of foundation denotes the reaction per unit length when the deflection is set equal to one. Bradbury theorized that a dowel bar encased in concrete will behave as a beam on an elastic foundation (7). Using Bradbury's assumption, a dowel bar encased in concrete will deflect in the same manner as a beam resting on an elastic foundation. Figure 2.1 illustrates the deflection of a dowel bar encased in concrete, based on the deflection of a beam on an elastic foundation.

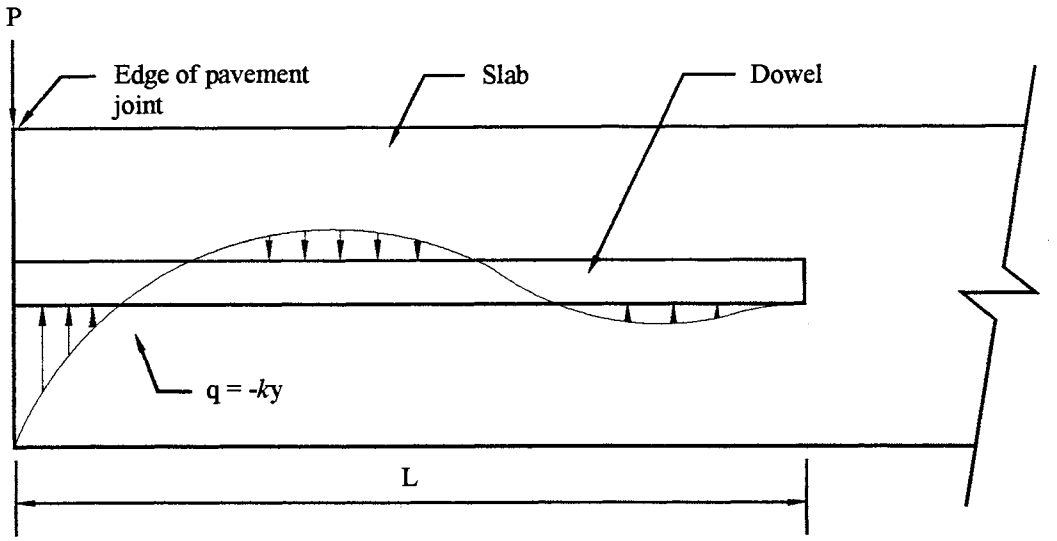

Figure 2.1 Pressure distribution from deflected dowel bar

The general solution to Timoshenko's differential equation is found in Equations 2.2 and 2.3 (8).

$$y_o = e^{\beta x}(A \cos \beta x + B \sin \beta x) + e^{-\beta x}(C \cos \beta x + D \sin \beta x) \quad (2.2)$$

where,

$$\beta = \sqrt[4]{\frac{k}{4EI}} = \text{relative stiffness of the beam on the elastic foundation (in.}^{-1}) \quad (2.3)$$

k = modulus of foundation (psi)

By applying the appropriate boundary conditions for any given problem the constants A, B, C, and D can be determined. Once these constants are determined a deflection equation along the entire length of a beam can be developed. For a semi-infinite beam with a moment, M_0, and a point load, P, Equation 2.2 equivalent to Equation 2.4.

$$y = \frac{e^{-\beta x}}{2\beta^3 EI}[P \cos \beta x - \beta M_o(\cos \beta x - \sin \beta x)] \quad (2.4)$$

Integrating Equation 2.4 will yield the slope of the beam, as shown in Equation 2.5.

$$\frac{dy}{dx} = \frac{e^{-\beta x}}{2\beta^2 EI}\left[(2\beta M_o - P)\cos \beta x - P \sin \beta x\right] \tag{2.5}$$

2.2.1.2 Friberg's Analytical Model

Friberg applied Timoshenko's elastic foundation theory to a beam of semi-infinite length (9). By assuming that the inflection point exists at the center of the joint, Equations 2.4 and 2.5 can be solved. This solution will be shown in detail in Chapter 5; using the aforementioned assumption, Equation 2.4 becomes Equation 2.6.

$$y_o = \frac{P}{4\beta^3 EI}(2 + \beta z) \tag{2.6}$$

where,

$$\beta = \sqrt[4]{\frac{K_o b}{4EI}} = \text{relative stiffness of the dowel bar encased in concrete (in.}^{-1}\text{)} \tag{2.7}$$

K_o = modulus of dowel support (pci)
b = dowel bar width (in.)
E = modulus of elasticity of the dowel bar (psi)
I = moment of inertia of the dowel bar (in.^{4})
P = load transferred through the dowel bar (pounds)
z = joint width (in.)

Friberg used the modulus of dowel support, K_o, in his equation. The modulus of dowel support is the reaction per unit area causing a deflection equal to one. Friberg used the expression $K_o b$ to replace the modulus of foundation, k, from Timoshenko's model. Friberg's equation was developed using a semi-infinite dowel length. Dowel bars have a finite length so this equation would not apply to dowel bars used in practice today. However, Porter et al. has shown that Friberg's equation can be used with little to no error if the βL value is greater than two (10, 11). Where the length, L, is taken to be the length of the dowel bar embedded in concrete, or approximately one-half the dowel bar length.

2.3 Pavement Joint Deflection

2.3.1 Relative Deflection Across a Pavement Joint

The relative deflection across a pavement joint, Δ, consists of four separate components. These components, as shown in Figure 2.2, consist of the deflection of the dowel at each joint face, the deflection due to the slope of the dowel bar, shear deflection, and flexural deflection. When considering all possible components for relative deflection the following expression in Equation 2.8 is found.

$$\Delta = 2y_o + z\left(\frac{dy_o}{dx}\right) + \delta + \frac{Pz^3}{12EI} \tag{2.8}$$

where,

y_o = deflection at the face of the joint (in.)
$\delta = \frac{\lambda Pz}{AG}$, shear deflection (in.) (2.9)
P = load transferred by dowel bar (pounds)
λ = form factor
A = cross-sectional area of the dowel bar ($in.^2$)
G = shear modulus (psi)

In this research, a joint width of 1/8 in. was used for the specimens. Using such a small joint width allows the deflection due to the slope of the dowel bar to be approximately equal to zero, which is the case in the author's research since the width and the slope of the joint are small. This small joint width also means that the flexural deflection is approximately equal to zero since the joint width term is cubed. After removing both the slope and flexural deflections from Equation 2.8, Equation 2.10 remains.

$$\Delta = 2y_o + \delta \tag{2.10}$$

Solving Equation 2.10 for y_o yields Equation 2.11.

$$y_o = \frac{\Delta - \delta}{2} \tag{2.11}$$

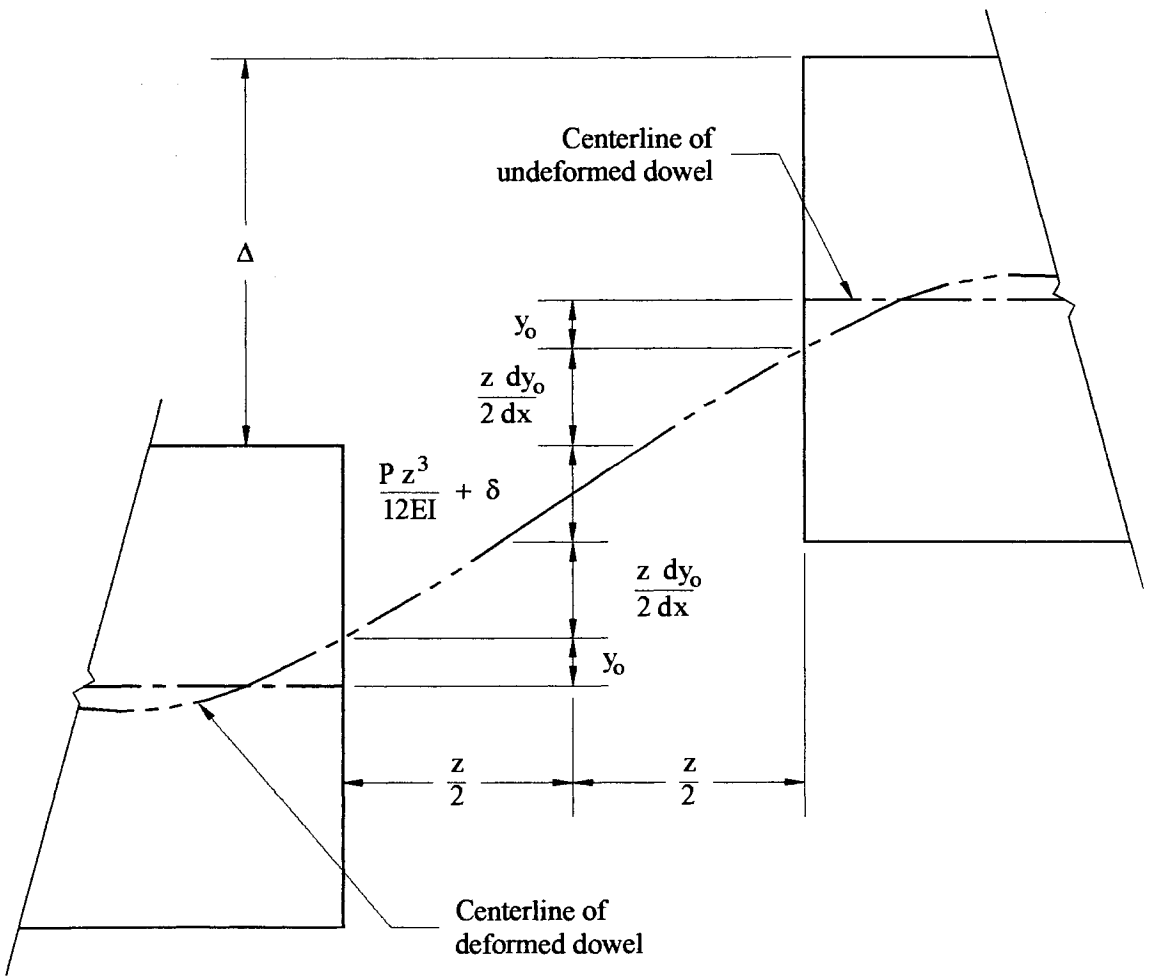

Figure 2.2 Relative deflection between adjacent pavement slabs (12)

As was stated previously, the deflection due to the slope of the dowel bar has been neglected in previous research at ISU because of the small joint width used with the specimens. Numerically, the deflection due to the slope of the dowel bar can be calculated to

be insignificant to the results. However, consideration needs to be given as to when the deflection due to the slope of the dowel bar needs to be addressed. Theoretical investigation on this topic will be presented in a later chapter.

2.3.2 Form Factor and Shear Deflection

As was shown in Equation 2.9, one variable used in determining shear deflection is the form factor, λ. The form factor can be defined as the ratio of the strain energy caused by the actual shear-stress distribution to the strain energy caused by a constant shear-stress distribution. This only applies to loads that cause a fiber stress inside the elastic limit. According to Serra-Conrads (13), the form factor can be determined by using the common shear stress equation shown in Equation 2.12.

$$\tau = \frac{PA'y'}{It(y)} \tag{2.12}$$

where,

τ = horizontal shear stress in the dowel bar (psi)

A' = cross-sectional area at location of shear stress to edge of member (in^2.)

y' = distance from neutral axis to the centroid of the area A' (in.)

$t(y)$ = width of the dowel bar (in.)

Inserting the shear stress of the section into the equation for the variation in strain energy returns Equation 2.13.

$$d(\Delta U) = \iint_{LA} \frac{\tau^2}{2G} dAdL \tag{2.13}$$

where,

ΔU = Variation in strain energy (lb-in./$in.^3$)

Equation 2.13 can be integrated to find the strain energy. The general strain energy equation is shown in Equation 2.14.

$$U = \lambda \int_{L} \frac{P^2}{2AG} dL \tag{2.14}$$

where,

U = Strain energy (lb-in./in.^{3})

Equation 2.15 relates Equation 2.14 to Equation 2.9. Equation 2.15 is based on Castigliano's Theorem (14).

$$\delta = \frac{\partial U}{\partial P} \tag{2.15}$$

According to Young (14), a solid circular cross-section has a form factor of 10/9 while a solid rectangular cross-section has a form factor of 6/5. The dowel bars used in this research consist of round bars, elliptical bars, and "shaved" bars. All the cross-sections of these bars will fall between a rectangular section and a circular section. In this research, the amount of total deflection contributed by shear deflection was very small due to the small joint width of 1/8". While changing the form factor has some influence on the shear deflection value, the change has little to no effect on the deflection at the face of the joint, the modulus of dowel support or the concrete bearing stress values. Therefore, to simplify the calculations, a form factor of 10/9 was used for all dowel bars in this research.

2.4 Theoretical Bearing Stress

The bearing stress on the concrete at the face of the joint is critical for proper function of the dowel bar in the concrete. If the bearing stress on the concrete becomes too large the concrete will begin to break away, or crush, where in contact with the dowel bar. Repetitive high stress loadings of the dowel bar-concrete interface will create a void. This void creates an additional amount of deflection in the system before the dowel bar will begin to take on the load applied. This additional deflection creates a loss in the efficiency of the dowel bar to

transfer load across the joint. This loss in efficiency must now be carried by the subgrade, which puts additional stress on the subgrade and creates the possibility for differential settlement of adjacent slabs.

If the dowel behaves as a beam on an elastic foundation, the bearing stress at the face of the joint, σ_b, is proportional to the deflection at the face of the joint. This relationship for Timoshenko's model is expressed using Equation 2.15.

$$\sigma_{bT} = ky_o \tag{2.16}$$

The bearing stress for Friberg's model is expressed in Equation 2.16.

$$\sigma_{bF} = K_o y_o \tag{2.17}$$

The bearing stress on the concrete needs to be kept low to make certain that no crushing of the concrete or oblonging of the dowel bar encasement occurs. An important note is that the Timoshenko and Friberg bearing stresses are in different units. The Timoshenko bearing stress is force per unit length, while the Friberg bearing stress is in terms of force per unit area. The next section will discuss why this difference exists.

2.5 Modulus of Foundation versus Modulus of Dowel Support

The difference between Timoshenko's and Friberg's models is reflected in the β term in the deflection equation, more specifically, Equations 2.3 and 2.7, which are repeated here for convenience.

$$\beta = \sqrt[4]{\frac{k}{4EI}} = \text{relative stiffness of the beam on the elastic foundation (in.}^{-1}\text{)} \tag{2.3}$$

$$\beta = \sqrt[4]{\frac{K_o b}{4EI}} = \text{relative stiffness of the dowel bar encased in concrete (in.}^{-1}\text{)} \tag{2.7}$$

As was discussed previously, Friberg's $K_o b$ term is the equivalent to Timoshenko's k term. By definition the modulus of foundation differs from the modulus of dowel support solely by units.

The first equation discussed to determine the deflection of a beam on an elastic foundation, Equation 2.1, is based on the modulus of foundation. Later when Friberg modified Timoshenko's equation, the b-term, bar width, was added for the sole purpose of converting Timoshenko's modulus of foundation term from pounds per square inches into the pounds per cubic inches seen in the modulus of dowel support. This conversion was done to arrive at a convenient unit of stress when comparing the dowel bar bearing stress to concrete strength.

The bearing stress on the concrete needs to be kept low to make certain that no crushing of the concrete occurs. According to the American Concrete Institute's (ACI) Committee 325, the allowable bearing stress on the concrete is equivalent to Equation 2.18 (15).

$$\sigma_a = \left(\frac{4-b}{3}\right) f'_c \tag{2.18}$$

where,

σ_a = allowable bearing stress (psi)
b = dowel bar width (in.)
f'_c = compressive strength of concrete (psi)

This equation is applicable to dowel bars ranging in size from 0.75 in. to 2 in. and provides a factor of safety of approximately three.

3.0 EXPERIMENTAL INVESTIGATION

3.1 Introduction

The experimental data used in this paper was taken from recently completed research as well as past research conducted at ISU. All data utilized in this paper was part of research done for the Iowa Department of Transportation (IDOT) TR-408 "Investigation of Glass Fiber Composite Dowel Bars for Highway Pavement Slabs" project (12) and the American Highway Technology (AHT) "Dowel Bar Optimization" project (16). Both of the projects were conducted to analyze bearing stress on dowel bars of different materials and shapes.

3.2 Test Methods

Since the testing was conducted over an extended period of time, different testing methods were developed and utilized. With the collection of data, problems with the current test method were determined and new approaches to future testing were developed and employed. While the changing of test methods was done to decrease the error in the testing, this change can also lead to confusion. This section will discuss the individual test methods and the dowel bars tested with each method.

3.2.1 Iosipescu Test Method

According to Walrath and Adams (17), the Iosipescu test achieves a state of pure shear loading at the centerline of the specimen because of the specimen's geometry. Figure 3.1 shows the original Iosipescu test developed by Walrath and Adams. Figure 3.2 shows the Iosipescu shear test specimen. To use the Iosipescu shear test method, a test frame was used that had been previously constructed for ISU research (11) and was based on smaller Iosipescu test frames developed by Adams. The test frame for testing Iosipescu specimens

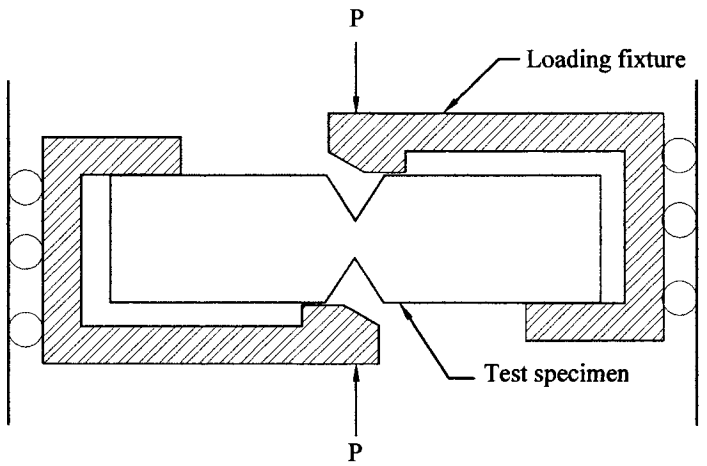

Figure 3.1 Iosipescu test designed by Adams and Walrath (12)

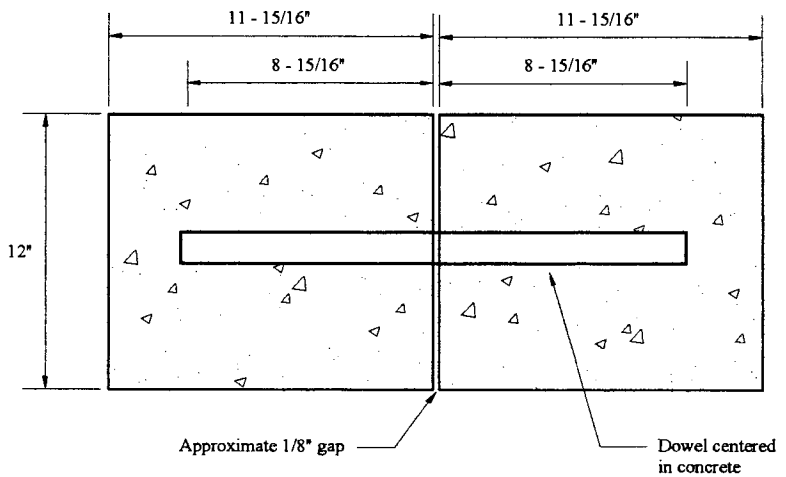

Side View

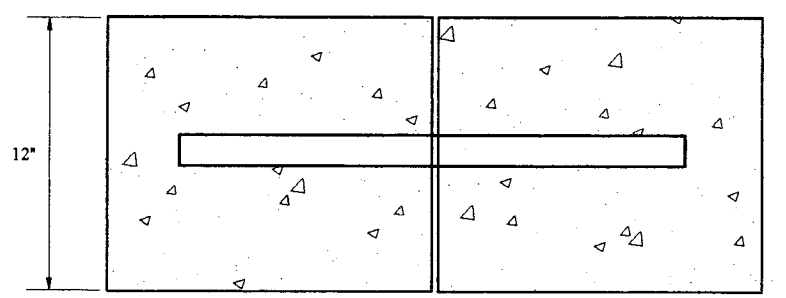

Top View

Figure 3.2 ISU Iosipescu shear test specimen (12)

is shown in Figure 3.3. The dowel-concrete system is held tight by the tension rods to minimize bending and rotation. One end of the specimen is fixed and the other end is

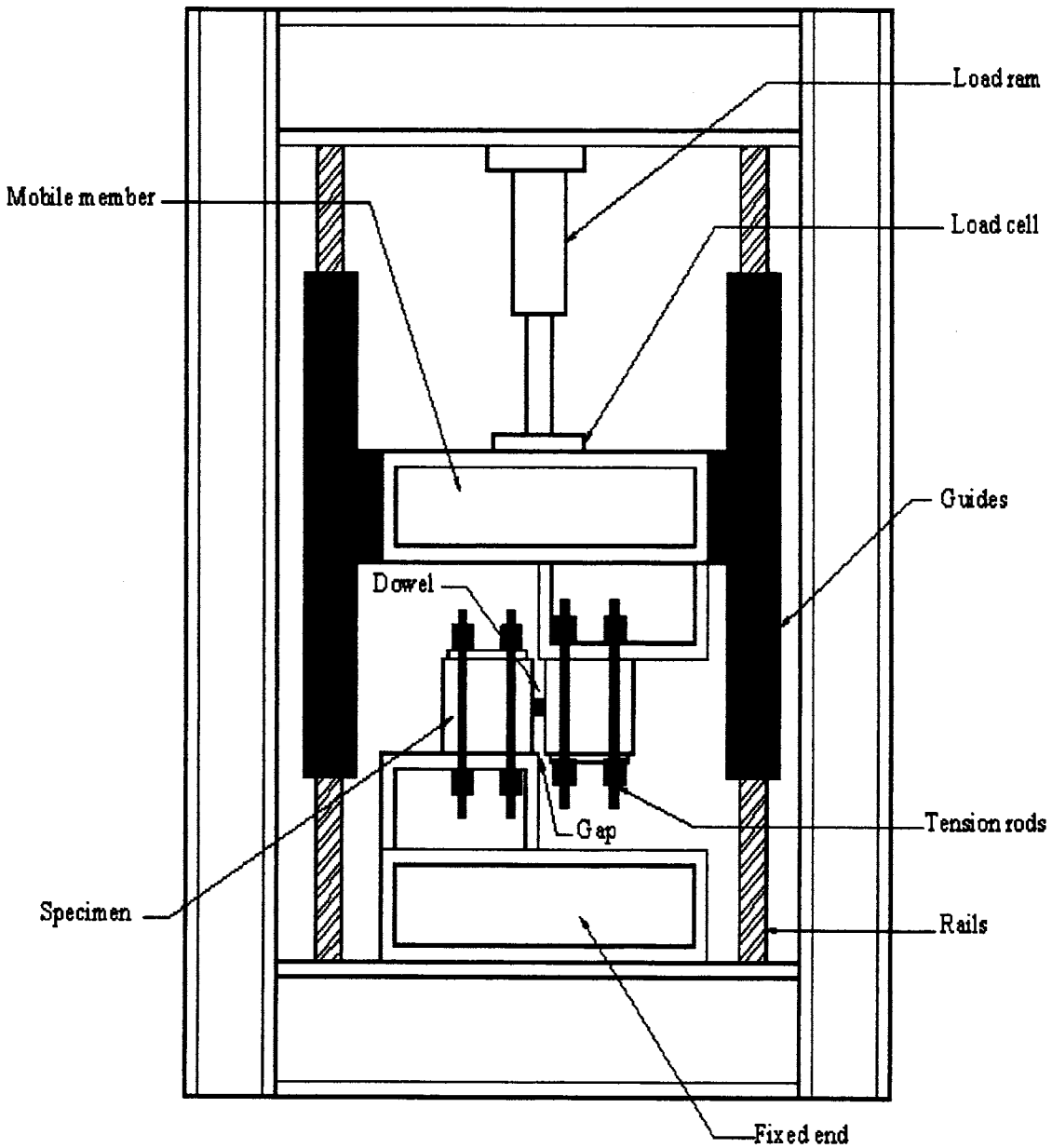

Figure 3.3 ISU Iosipescu testing frame (12)

movable. This set-up allowed the load to be transferred as would be seen in the field resulting in direct shear of the dowel. The gap shown in Figure 3.2 allows the load to be transferred from one side of the specimen to the other without having aggregate interlock or interface friction taking some of the load.

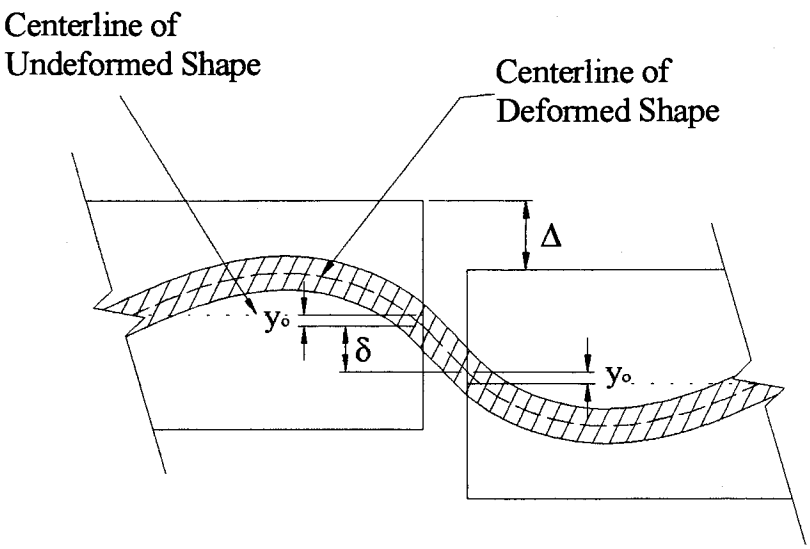

Figure 3.4 Differential deflection at a contraction joint (12)

3.2.2 AASHTO Shear Test Method

The American Association of State Highway and Transportation Officials (AASHTO) shear testing procedure applies loading to the dowel bars in a very similar manner as the Iosipescu shear test method. The major differences are the specimen and testing set up. The shear test method used for this research was based on the AASHTO T253-76 (18) standard test method. There are two dowels encased in concrete, which simulates two 12-in. high contraction joints. The test specimen is shown in Figure 3.5. The AASHTO test applies a uniform load as shown in Figure 3.6 to the middle concrete block. The deflected shape of the AASHTO specimen is also shown in Figure 3.6. The dowel bar

encased within the concrete block deflects similarly to the specimen shown in Figure 3.4. For tests conducted at ISU (12, 16), the AASHTO setup was modified slightly. In the modified setup, the joints were shortened to simplify the analysis. The modified joint width was changed to 1/8-in. contraction joints rather than the 3/8-in. contraction joints used by AASHTO. The beam width was also changed from 12 in. to 10 in.

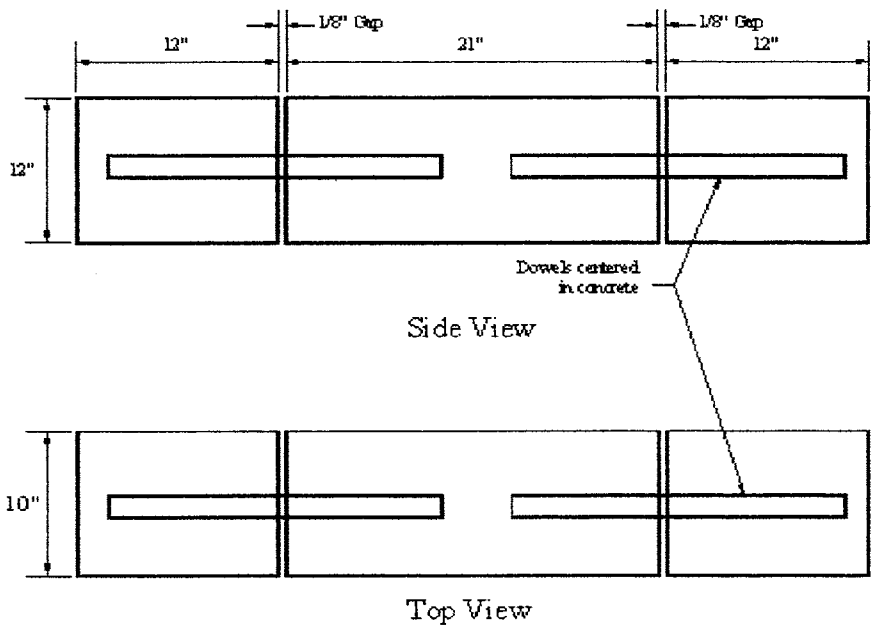

Figure 3.5 Modified AASHTO T253 test specimen (12)

As was done in the Iosipescu specimens, the AASHTO specimens also require that the load-deflection characteristics were known to be able to calculate the modulus of dowel support or the modulus of foundation. Equation 2.9 is still used to calculate the differential deflection as was discussed in Section 3.2.1 with the Iosipescu specimen.

3.2.3 Elemental Fatigue Test Method

3.2.3.1 Test Procedure

As outlined in Section 3.2.2, a modified AASHTO test was used for a portion of the direct shear testing. This test was slightly modified and a special test frame was constructed for use in the elemental fatigue testing. The only modification made to the previously discussed AAHSTO method was a change in the loading. In the static shear test, a uniform load was applied to the center block, as shown in Figure 3.6. A change from the uniform load

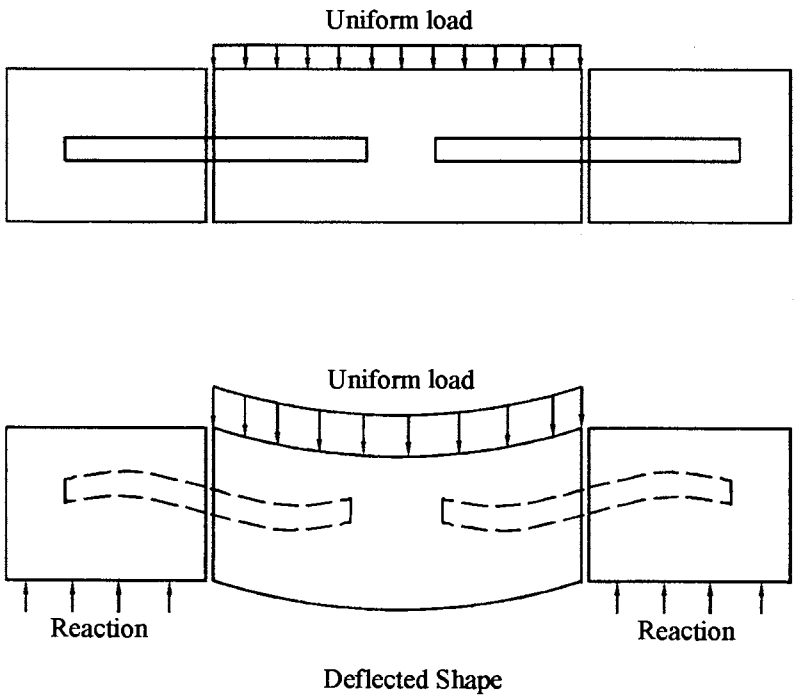

Figure 3.6 Uniform load applied to AASHTO shear specimen

to point loads was made in the fatigue test so clamps could be attached to the center block and the actuator could press down on the specimen as well as apply an upward force. The positioning of the two clamps near the ends of the center block was also done to decrease the deflection in the center of the block and force the inflection point towards the center of the

joint. This reversal of load was used to subject the dowel bars to a stress reversal, as is experienced when the wheel load passes over the joint. A test setup of this procedure is shown in Figures 3.7 and 3.8. The elemental fatigue testing was only used in the IDOT investigation.

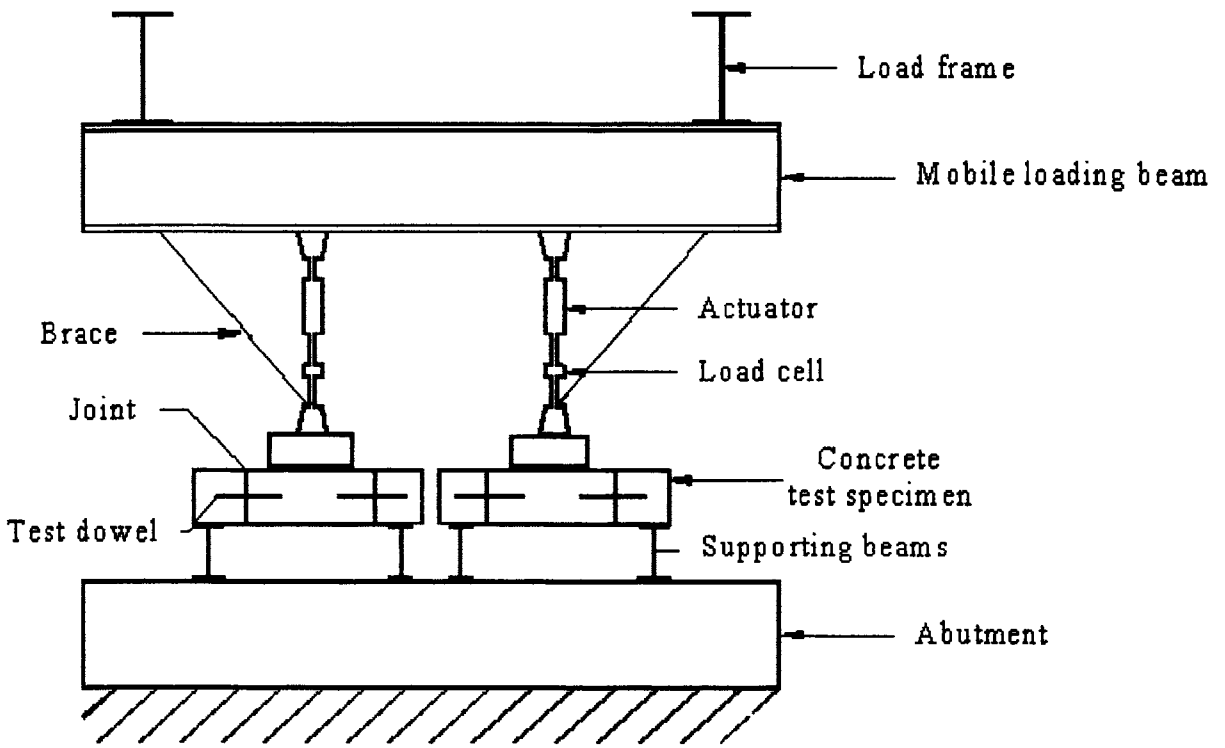

Figure 3.7 Testing frame for elemental fatigue test (12)

3.2.3.2 Loading

The loading actuators shown in Figure 3.7 applied a load of 3300 pounds to each specimen. This loading is the equivalent of 1650 pounds on each dowel bar and is closely related to what the critical dowel would experience on a 12-in. slab with the dowel bars spaced at 12 in. center to center. A deflection versus load diagram was taken before any fatiguing of the specimen had occurred. The specimen was then tested for 1 million cycles at a rate of approximately 4 cycles per second. After the specimen had seen one million cycles, a second deflection versus load diagram was developed. The two deflection versus load diagrams were used to calculate the modulus of dowel support and modulus of foundation for the dowel bar before and after fatiguing.

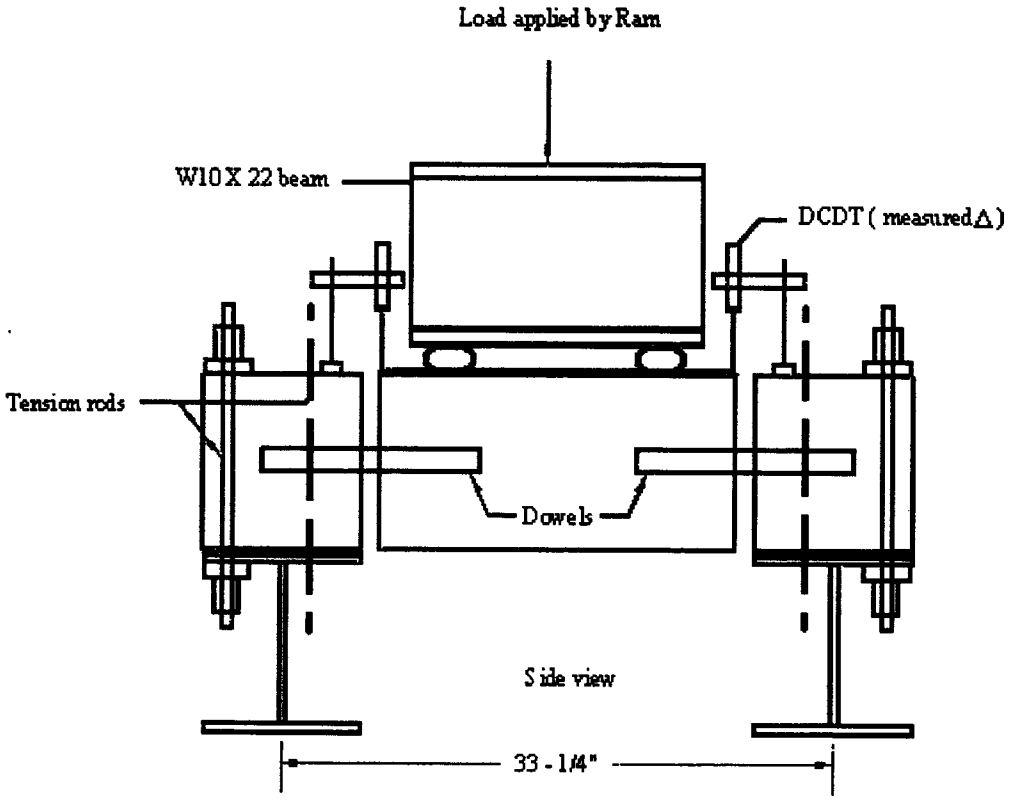

Figure 3.8 Loading of elemental fatigue specimen (12)

3.2.4 Elemental Direct Shear Test Method

The elemental specimens were constructed as a modified AASHTO T253 specimen (16) with the same dimensions as the specimen for the AASHTO shear test method, as was shown in Figure 3.5. A 1/8-in. gap was used to simulate a field pavement as well as aid in the reduction of flexure across the joint. As with the AASHTO shear test, the dowel bars were placed at mid-height of the specimen.

The testing of the direct shear specimens was conducted on a 400-kip capacity SATEC 400HVL universal-testing machine at the ISU structures laboratory. A modified AASHTO T253-76 test was used for testing the elemental direct shear specimens. This procedure requires that the end blocks of the specimens be clamped so that no rotation is allowed. Before testing began, the specimens were preloaded. The preloading procedure consisted of loading the direct shear specimens five times at a rate of 2000 pounds/min until 5,000 pounds was reached. This procedure was used to help settle the specimens so that more accurate results would be obtained. With the end blocks restrained from rotation, a load of 2000 pounds/minute was applied to the middle section of the specimen while deflection on each end was measured. Figure 3.9 shows how the load was applied to the center section of the specimen. The deflections that were measured were the relative deflections across the joint, or rather the deflections from the stationary end blocks to the deflecting center block. The deflections were measured by using Direct Current Displacement Transducers (DCDT's), see Figure 3.8. Measurements of deflection and corresponding load were taken every two seconds. The tests were carried out on all specimens until a load of 10,000 pounds was reached. This data was then used to create a

load vs. deflection diagram. This procedure has been tested and validated as an acceptable approach by Rohner (19).

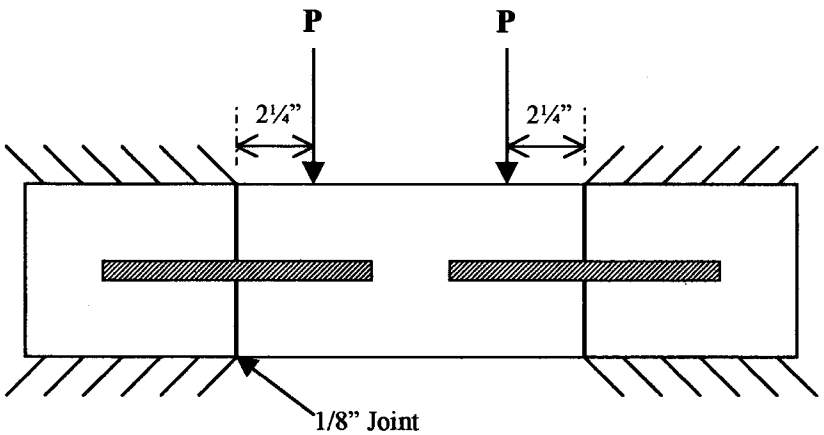

Figure 3.9 Location of load on direct shear specimen

While testing the first two direct shear specimens, a problem was encountered. While preparing the initial specimens for testing, the author observed that the specimens were not sitting level in the testing apparatus. The decision was made to conduct the first test and attach two DCDT's to the rear of both end blocks. The end block DCDT's were mounted to measure the movement of the end blocks opposite the dowel bars, or to check the end blocks for rotation. After performing tests on the first two direct shear specimens, the DCDT's revealed that there was a significant amount of rotation occurring on the end blocks.

This rotation was due to the unevenness of the bottom of the specimens. The forms used to cast the specimens were not perfectly flat which created unevenness along the bottom of the specimen. This unevenness on the bottom of the specimens caused the specimen to shift when loaded. As more load was applied, more movement of the end blocks would

occur. The solution to this problem was to cast the bottom of the end blocks in dental plaster. The plaster that was used for this procedure was Labstone, which had a compressive strength of 8000 psi. Upon retests of the two initial direct shear specimens, the rotation was again monitored and no measurable amount of rotation was seen. All of the remaining direct shear specimens were cast in the Labstone to be sure that the bottoms remained level during testing. As a precaution, rotation readings were taken for all the direct shear specimens to ensure that no rotation occurred on any of the remaining specimens. The direct shear method was only used in the AHT investigation (16).

3.3 Aged Specimens

"Aged" specimens were constructed indentically as the modified AASHTO shear specimens. After allowing the specimens to cure for 28 days, they were placed in a 131.3°F solution of sodium hydroxide and satuarated calcium hydroxide with a pH of 12.0-12.5 for 99 days. This aging is equivilent to 18,247 days or approximately 50 years of real time aging according to work done by Boris (20). The testing for each aged specimen was identical to the testing for the unaged specimen of each type. Aged specimens were only tested with the modified AASHTO shear method and the elemental fatigue method.

3.4 Iowa Department of Transportation Investigation

The static tests used in this investigation were the Iosipescu Test method and the AASHTO Shear Test method, as shown in Figures 3.3 and 3.6. Epoxy-coated steel dowel bars are the most common dowel bars used in highway pavements today. Therefore, the dowel bar materials chosen should somehow relate back to the standard dowel bars. This relation was accomplished by using two different aluminum and copper dowel bars. The aluminum and copper dowel bars were chosen due to their different modulus of elasticity, E.

One aluminum and one copper dowel bar each had a diameter of 1.5 in. and a second bar diameter was selected that gave both materials the same modulus of rigidity, EI, as that of the standard epoxy-coated steel dowel bar. Two different sizes of GFRP dowels were also used. Table 3.1 shows the different sizes and the material properties of the different dowel bars. The properties for the steel, aluminum, and copper shown in Table 3.1 were obtained from Ugural's textbook (21).

The concrete strengths were to represent the strength that a pavement would typically experience. The target concrete mix strength was 6000 psi for each set of dowel bars shown in Table 3.1. Once the concrete reached the desired strength, the specimens were tested.

Table 3.1 Dowel material and sizes used in IDOT investigation

Material	Diameter, in.	E, (10^6) psi	EI, (10^6) lb-in.^{2}
Epoxy-Coated Steel	1.5	29	7.206
Stainless Steel	1.5	28	6.958
Plain Steel[a]	1.5	29	7.206
Aluminum[b]	1.5	10	2.485
	1.957		7.200
Copper[b]	1.5	17	4.225
	1.714		7.202
GFRP	1.5	4.93[d]	1.225
GFRP[b]	1.75	6.20[c]	2.854
GFRP	1.875	6.51[d]	3.950

[a] Plain Steel indicates an epoxy-coated dowel bar with the coating removed.
[b] These dowel bars were only tested in unaged specimens.
[c] Properties were taken from work done by Porter et al. (22) and (23).
[d] Properties were taken from work done by Porter et al. (12).

The dowel bars evaluated in the elemental fatigue tests consisted of bars that were made out of varying shapes and materials. Three types of dowel bars tested in the fatigue test

were also tested in the static test. There were also two additional, alternatively shaped dowel bars tested, an elliptical and a shaved dowel bar. The dimensions of these alternatively shaped dowel bars can be seen in Figure 3.10. Table 3.2 shows the different shapes and materials that were used in the elemental fatigue testing.

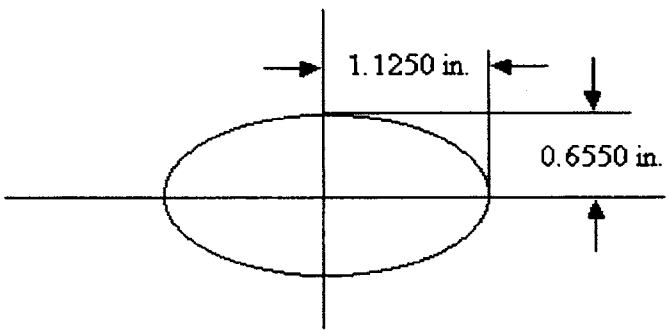

Alternate Shape #1: Ellipse

Equation of the Ellipse: $\frac{x^2}{1.125^2} + \frac{y^2}{0.655^2} = 1$

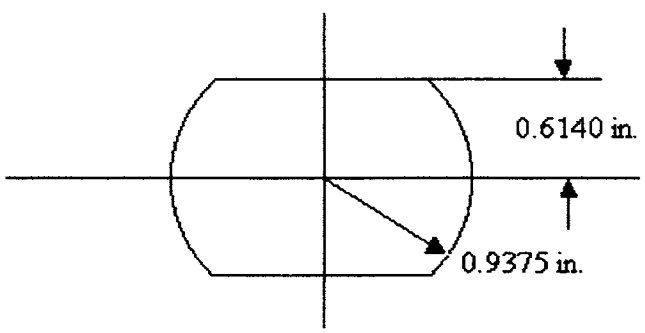

Alternate Shape #2: Originally a 1.875-in. diameter dowel bar with the top and bottom halves shaved. The corners have a fillet with a radius of 0.15 in.

Figure 3.10 Alternatively shaped dowel bars

Table 3.2 Dowel material and sizes used in Elemental Fatigue testing

Material	Diameter, in.	E, (10^6) psi	EI, (10^6) lb-in.^{2}
Epoxy-Coated Steel	1.5	29	7.206
Stainless Steel	1.5	28	6.958
Elliptical GFRP[a]	1.31[c]	8.66	2.210
Shaved GFRP[a b]	1.23[c]	6.51	1.619
GFRP	1.5	4.93[d]	1.255
GFRP	1.875	6.51[d]	3.950

[a] These dowel bars were only tested in unaged specimens.
[b] The Shaved GFRP dowel bars were cut from the 1.875-in. diameter dowel bars.
[c] Dimensions listed are the minor axis dimension. See Figure 3.11 for an illustration of these dowel bars.
[d] Properties were taken from work done by Porter et al. (12).

3.5 American Highway Technology Investigation

In the AHT investigation, the Elemental Direct Shear Test Method, outlined in Section 3.2.4, was utilized. The purpose of this research was to determine the effect that dowel bar shape and size had on bearing stress, σ_b, at the face of the joint. In this research there were five different types of dowel bars tested. Ten dowel bars of each dowel bar type were used. Two dowel bars were placed in each specimen, which required the construction of 25 concrete specimens, five specimens for each type of dowel bar. The different types of dowel bars were:

- 1.25-in. diameter epoxy-coated steel,
    - Area = 1.227 in.^{2}
- 1.5-in.diameter epoxy-coated steel,
    - Area = 1.767 in.^{2},
- large elliptical steel (major axis = 1.98 in.: minor axis = 1.34 in.),
    - Area = 2.084 in.^{2}

- medium elliptical steel (major axis = 1.66 in.: minor axis = 1.13 in.),
    - Area = 1.473 $in.^2$
- small elliptical steel (major axis = 1.41 in.: minor axis = 0.88 in.).
    - Area = 0.975 $in.^2$

See Table 3.3 for a test matrix of the specimens tested.

Table 3.3 Test matrix of AHT test specimens

Description of Dowel Bar	Number of Test Specimens	Number of Dowel Bars
1.25"ϕ Epoxy-Coated steel	5	10
1.5"ϕ Epoxy-Coated steel	5	10
Large Elliptical Steel	5	10
Medium Elliptical Steel	5	10
Small Elliptical Steel	5	10

4.0 ANALYSIS OF EXPERIMENTAL RESULTS

4.1 Introduction

The tests outlined in Chapter 3 were followed and the appropriate deflection data was gathered. This deflection data was then utilized to calculate the modulus of dowel support and the modulus of foundation, as described in Chapter 2. This chapter will outline the modulus values that were acquired for each specimen as well the associated bearing stress.

4.2 Iowa Department of Transportation Results

The following section will detail the experimental data that was calculated for the IDOT project.

4.2.1 Iosipescu Test Method & AASHTO Shear Test Method

From the actual deflection versus load diagrams that were created during testing, linear regression was used to determine a load-deflection equation for each specimen. Using this relationship, a relative deflection was obtained for a dowel load of 2,000 pounds. A 2,000-pound load represents the maximum load that the critical dowel in a typical pavement would be expected to experience due to the distribution of a 9,000-pound wheel load (12). The deflection at the face of the joint, y_o, was determined in Equation 2.11, repeated here for convenience. The equation for shear deflection, δ, is shown in Equation 4.1 and was obtained from Young (14).

$$y_0 = \frac{\Delta - \delta}{2} \tag{2.11}$$

$$\delta = \frac{10 \cdot P \cdot z}{9 \cdot G_{xy} \cdot A} \tag{4.1}$$

Table 4.1 gives the average total relative deflection, average shear deflection, and average deflection at the face of the joint for each type of dowel bar using an Iosipescu shear

test. Table 4.2 is a listing of the average total relative deflection, average shear deflection, and average deflection at the face of the joint using the modified AASHTO direct shear test. The values in both tables were calculated for a 2000-pound load and are for unaged specimens. Note that the 1.75-in. diameter GFRP dowel bar was replaced with a 1.875-in. diameter GFRP dowel bar in later research.

Table 4.1 Iosipescu Test – **Unaged** - Average relative deflection, shear deflection, and deflection at face of joint.

Dowel Bar	**Average Δ, in.***	**Average δ, in.***	**Average y_o, in.***
1.5"ϕ Epoxy-Coated	0.003211	0.000014	0.001599
1.5"ϕ Stainless Steel	0.003600	0.000015	0.001793
1.5"ϕ Plain Steel	0.002699	0.000014	0.001343
1.5"ϕ GFRP	0.006137	0.000679	0.003035
1.75"ϕ GFRP[a]	0.007637	0.000242	0.003698

[a] Properties were taken from work done by Porter et al. (11).

*Note: The deflections cannot be measured this accurately, but are needed to display the effects of shear deflection.

Table 4.2 Modified AASHTO Test – **Unaged** - Average relative deflection, shear deflection, and deflection at face of joint.

Dowel Bar	**Average Δ, in.***	**Average δ, in.***	**Average y_o, in.***
1.5"ϕ Epoxy-Coated	0.005426	0.000014	0.002706
1.5"ϕ Aluminum	0.009710	0.000041	0.004835
1.957"ϕ Aluminum	0.007901	0.000024	0.003938
1.5"ϕ Copper	0.006512	0.000024	0.003244
1.714"ϕ Copper	0.005415	0.000018	0.002698
1.5"ϕ GFRP	0.010810	0.000679	0.005065
1.875"ϕ GFRP	0.007472	0.000319	0.003576

*Note: The deflections cannot be measured this accurately, but are needed to display the effects of shear deflection.

Table 4.3 shows the average total relative deflection, average shear deflection, and average deflection at the face of the joint for each type of dowel bar using an Iosipescu shear test for the aged specimens. The values were calculated for a 2,000-pound load. This information corresponds to the unaged Iosipescu test results that are given in Table 4.1. There were no aged specimens tested using the modified AASHTO static test method.

Table 4.3 Iosipescu Test – **Aged** - Average relative deflection, shear deflection, and deflection at face of joint.

Dowel Bar	**Average Δ, in.***	**Average δ, in.***	**Average y_o, in.***
1.5"ϕ Epoxy-Coated	0.003415	0.000014	0.001701
1.5"ϕ Stainless Steel	0.002978	0.000015	0.001482
1.5"ϕ Plain Steel	0.002729	0.000014	0.001358
1.5"ϕ GFRP	0.005863	0.000679	0.002592
1.875"ϕ GFRP	0.006606	0.000319	0.003144

*Note: The deflections cannot be measured this accurately, but are needed to display the effects of shear deflection.

With the deflections calculated, the next step is to calculate the modulus of dowel support and the modulus of foundation. The modulus of dowel support and the modulus of foundation are calculated using similar procedures. To calculate the modulus of dowel support and the modulus of foundation, Equation 2.6 is used. However, the difference, as was discussed earlier, is found in the β term. For the modulus of foundation, Equation 2.3 is used. When calculating the modulus of foundation, Equation 2.7 is utilized. Equations 2.6, 2.3 and 2.7 are repeated here for convenience.

$$y_o = \frac{P}{4\beta^3 EI}(2 + \beta z) \qquad (2.6)$$

where,

$$\beta = \sqrt[4]{\frac{k}{4EI}} = \text{relative stiffness of the beam on the elastic foundation (in.}^{-1}\text{)} \quad (2.3)$$

$$\beta = \sqrt[4]{\frac{K_o b}{4EI}} = \text{relative stiffness of the dowel bar encased in concrete (in.}^{-1}\text{)} \quad (2.7)$$

The appropriate values of k, or K_o, are imputed into Equation 2.6. After multiple values are imputed, a k versus y_o graph, or K_o versus y_o graph, can be created. Since Equation 2.6 is dependent on the bar shape and material properties, a graph must be created for each dowel bar of a different shape and/or material. Shown in Figure 4.1 is a sample k versus y_o graph for a 1.5-in.diameter round epoxy-coated steel dowel bar calculated at a 2000-pound load. Similarly, in Figure 4.2 is a sample K_o versus y_o graph for a 1.5-in. diameter round epoxy-coated steel dowel bar at a 2000-pound load. However, since there was a linear relationship between the load and the deflection, the results for the modulus of dowel support and modulus of foundation are not dependent on the load.

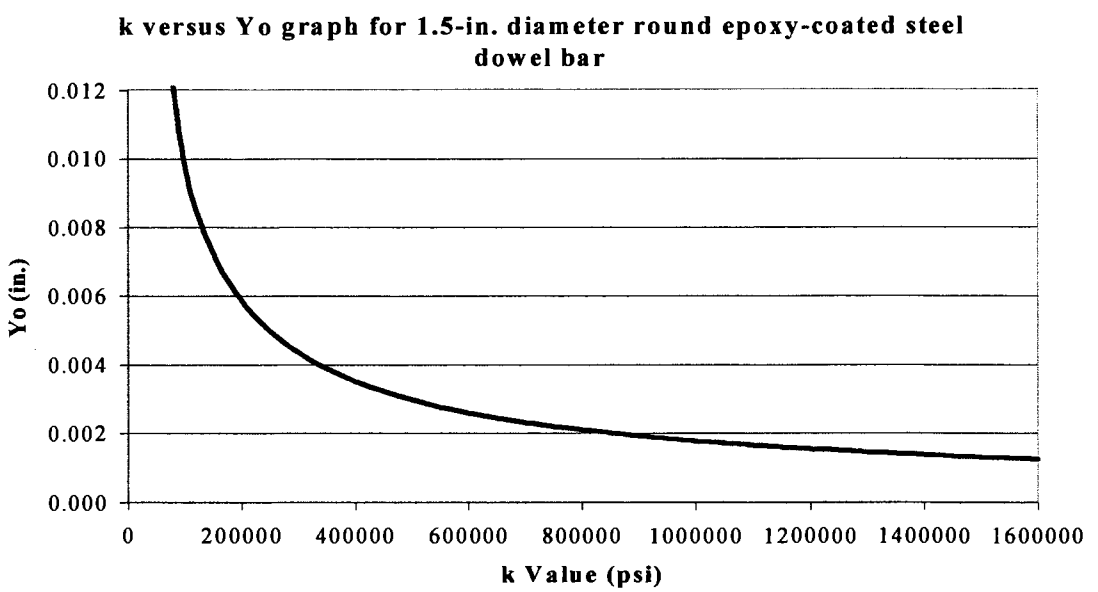

Figure 4.1 k versus y_o for a 1.5-in. diameter round epoxy-coated steel dowel bar at a 2000-pound load

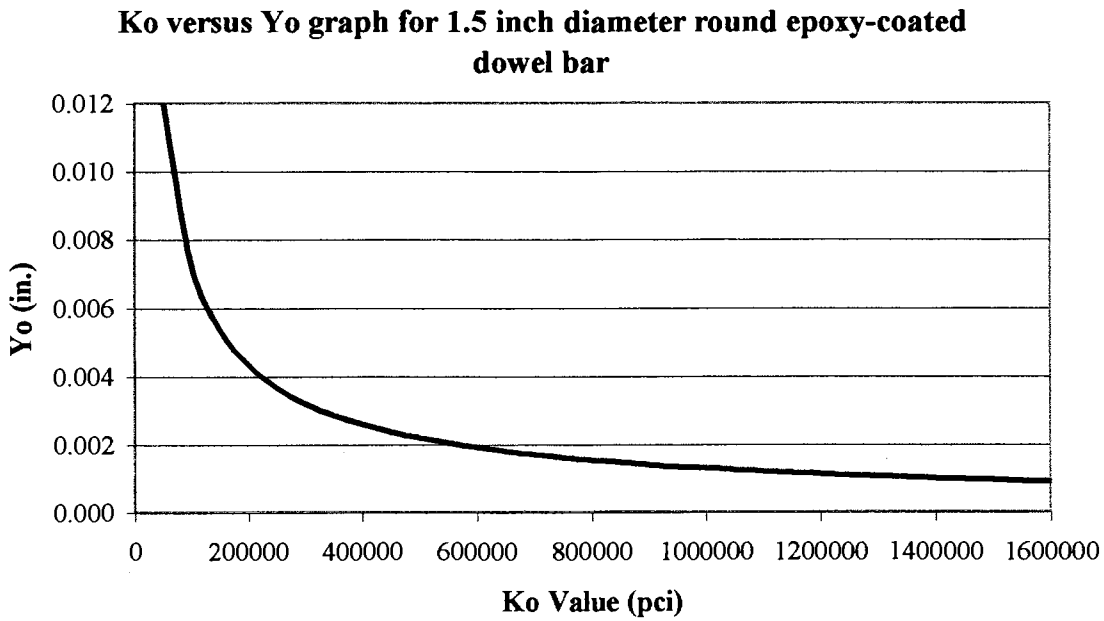

Figure 4.2 K_o versus y_o for a 1.5-in. diameter round epoxy-coated steel dowel bar at a 2000 -pound load

Using the modulus of foundation, or the modulus of dowel support, along with the deflection at the face of the joint, the concrete bearing stress can be calculated. These equations are repeated here for convenience.

$$\sigma_{bT} = ky_o \tag{2.16}$$

$$\sigma_{bF} = K_o y_o \tag{2.17}$$

Table 4.4 is a listing of each unaged specimen type and the associated average modulus of foundation and average modulus of dowel support. Table 4.5 shows the aged specimens values for average modulus of foundation and average modulus of dowel support. Again, the data in the following table has been calculated for a load of 2000 pounds. The results in Table 4.5 are from the Iosipescu test method since no aged specimens were tested using the modified AASHTO method.

Table 4.4 **Unaged** - Average modulus of foundation and modulus of dowel support values

Dowel Bar	Average k, psi	Average K_o, pci
Iosipescu		
1.5"ϕ Epoxy-Coated	1,149,275	772,330
1.5"ϕ Stainless Steel	996,630	665,170
1.5"ϕ Plain Steel	1,452,689	976,750
1.5"ϕ GFRP	897,498	598,443
1.75"ϕ GFRP	516,139	300,000
Modified AASHTO		
1.5"ϕ Epoxy-Coated	567,044	377,774
1.5"ϕ Aluminum	374,682	251,133
1.957"ϕ Aluminum	342,719	176,500
1.5"ϕ Copper	533,812	355,786
1.714"ϕ Copper	569,422	332,032
1.5"ϕ GFRP	450,023	299,847
1.875"ϕ GFRP	478,445	256,233

Table 4.5 Iosipescu Test - **Aged** - Average modulus of foundation and modulus of dowel support values

Dowel Bar	Average k, psi	Average K_o, pci
1.5"ϕ Epoxy-Coated	1,057,697	704,950
1.5"ϕ Stainless Steel	1,287,147	861,930
1.5"ϕ Plain Steel	1,431,183	954,071
1.5"ϕ GFRP	1,110,186	740,432
1.875"ϕ GFRP	568,835	303,404

As can be seen in Table 4.4, the values given for the modulus of foundation and the modulus of dowel support vary greatly between test methods. The reason for the lower modulii values with the modified AASHTO test method is most likely related to the rotation that the author observed while conducting his own research, as explained in Section 3.2.4.

The researcher responsible for the test data above did not check for rotation of the specimens and therefore some may have occurred and reduced the overall stiffness of the system. A lower stiffness would explain the large variation shown above.

Even with this large variation in the modulii, the bearing stresses determined are relatively close when comparing both test methods. Since the bearing stress is the primary concern in this research, the author felt that all of the values where appropriate to be used collectively in this report. However, due to the large difference in the modulii, the values of both test methods should only be used to show trends in the behavior of the dowel bars and the values from one test method should not be compared directly to the other test method. Table 4.6 shows the Timoshenko and Friberg bearing stresses for the unaged bars. While Table 4.7 shows the associated bearing stresses for the aged specimens.

Table 4.6 **Unaged** - Average bearing stress values

Dowel Bar	Average σ_{bT} , pli	Average σ_{bF}, psi
Iosipescu		
1.5"ϕ Epoxy-Coated	1,838	1,235
1.5"ϕ Stainless Steel	1,787	1,193
1.5"ϕ Plain Steel	1,951	1,312
1.5"ϕ GFRP	2,724	1,816
1.75"ϕ GFRP	1,909	1,109
Modified AASHTO		
1.5"ϕ Epoxy-Coated	1,534	1,022
1.5"ϕ Aluminum	1,812	1,214
1.957"ϕ Aluminum	1,350	695
1.5"ϕ Copper	1,732	1,154
1.714"ϕ Copper	1,536	896
1.5"ϕ GFRP	2,279	1,519
1.875"ϕ GFRP	1,711	916

Table 4.7 Iosipescu Test - **Aged** - Average bearing stress values

Dowel Bar	**Average σ_{bT} , pli**	**Average σ_{bF}, psi**
1.5"ϕ Epoxy-Coated	1,799	1,199
1.5"ϕ Stainless Steel	1,908	1,277
1.5"ϕ Plain Steel	1,944	1,296
1.5"ϕ GFRP	2,878	1,919
1.875"ϕ GFRP	1,788	954

When reviewing the bearing stresses, both the Timoshenko and Friberg stresses follow the same trends. For a given material, bearing stresses tend to be higher on the smaller bars and the bearing stress decreases as the size of the bar increases. This behavior can also be stated that the bearing stress is inversely proportional to the size of the dowel bar.

Another trend that can be seen is that the GFRP dowel bars tend to have higher bearing stresses than that of a similarly sized metal dowel bar. The higher bearing stress in the GFRP can be explained by looking at the bearing stress equations. The bearing stress is related to the modulii and the deflection at the face of the joint. The modulii and the deflection are both related to the stiffness of the material. The material properties of GFRP dowel bars create a dowel bar with less stiffness than a similarly sized metal dowel bar. Thus, higher bearing stresses are developed.

The final trend can be seen when comparing the Timoshenko bearing stress to that of the Friberg bearing stress. The Timoshenko bearing stresses are always higher than the Friberg bearing stresses. The difference between the Friberg bearing stress and the Timoshenko bearing stress is equal to the width of the bar. This difference follows the assumption used by Friberg that the bearing stress was constant across the width of the dowel bar.

4.2.2 Elemental Fatigue Test Method

The purpose of the elemental fatigue testing was to determine if there is a significant decline in the modulii for the different dowel bars tested due to fatigue. The trends seen with these results are to be used to determine if one dowel bar may be more resistant to oblonging of the concrete adjacent to the dowel bar. Using the test method outlined in Section 3.2.3 and the analysis procedure outlined in Section 4.2.1, the following results were obtained. The average relative deflection, shear deflection and the averaged deflection at the face of the joint can be seen in Tables 4.8 thru 4.11. Tables 4.8 and 4.9 show the results before any cycling of the specimens had occurred for unaged and aged specimens, respectively. While Tables 4.10 and 4.11 contain the results after 1 million cycles had been applied to the specimens for unaged and aged specimens, respectively. These tables were calculated for a load of 2000 pounds.

Table 4.8 Fatigue Testing – **Unaged, 0 Cycles** - Average relative deflection, shear deflection, and deflection at face of joint.

Dowel Bar	Average Δ, in.*	Average δ, in.*	Average y_o, in.*
1.5"ϕ Stainless Steel	0.001357	0.000015	0.000671
Elliptical GFRP	0.002729	0.000529	0.001100
Shaved GFRP	0.002778	0.000415	0.001181
1.5"ϕ GFRP	0.005542	0.000681	0.002431
1.875"ϕ GFRP	0.004424	0.000319	0.002052

*Note: The deflections cannot be measured this accurately, but are needed to display the effects of shear deflection.

The modulus of foundation and the modulus of dowel support that were calculated can be seen in Tables 4.12 thru 4.15. Tables 4.12 and 4.13 contain the results for the dowel bars at 0 cycles and Tables 4.14 and 4.15 show the results for the dowel bars at 1 million

cycles. Tables 4.12 and 4.14 list the results for unaged specimen while the other two tables show the results for aged specimens.

Table 4.9 Fatigue Testing – **Aged, 0 Cycles** - Average relative deflection, shear deflection, and deflection at face of joint.

Dowel Bar	Average Δ, in.*	Average δ, in.*	Average y_o, in.*
1.5"ϕ Epoxy-Coated	0.001889	0.000014	0.000937
1.5"ϕ Stainless Steel	0.002230	0.000015	0.001108
1.5"ϕ GFRP	0.003734	0.000681	0.001527
1.875"ϕ GFRP	0.004881	0.000319	0.002281

*Note: The deflections cannot be measured this accurately, but are needed to display the effects of shear deflection.

Table 4.10 Fatigue Testing – **Unaged, 1 Million Cycles** - Average relative deflection, shear deflection, and deflection at face of joint.

Dowel Bar	Average Δ, in.*	Average δ, in.*	Average y_o, in.*
1.5"ϕ Stainless Steel	0.001218	0.000015	0.000602
Elliptical GFRP	0.002357	0.000529	0.000914
Shaved GFRP	0.002791	0.000415	0.001188
1.5"ϕ GFRP	0.005277	0.000681	0.002298
1.875"ϕ GFRP	0.004515	0.000319	0.002098

*Note: The deflections cannot be measured this accurately, but are needed to display the effects of shear deflection.

Table 4.11 Fatigue Testing – **Aged, 1 Million Cycles** - Average relative deflection, shear deflection, and deflection at face of joint.

Dowel Bar	Average Δ, in.*	Average δ, in.*	Average y_o, in.*
1.5"ϕ Epoxy-Coated	0.003644	0.000014	0.001815
1.5"ϕ Stainless Steel	0.002503	0.000015	0.001244
1.5"ϕ GFRP	0.004404	0.000681	0.001861
1.875"ϕ GFRP	0.006761	0.000319	0.003221

*Note: The deflections cannot be measured this accurately, but are needed to display the effects of shear deflection.

Table 4.12 **Unaged, 0 Cycles** - Average modulus of foundation and modulus of dowel support values

Dowel Bar	Average k , psi	Average K_o , pci
1.5"ϕ Stainless Steel	3,730,165	2,492,740
Elliptical GFRP	2,862,277	1,282,372
Shaved GFRP	2,904,544	1,557,594
1.5"ϕ GFRP	1,210,416	807,378
1.875"ϕ GFRP	1,009,375	538,623

Table 4.13 **Aged, 0 Cycles** - Average modulus of foundation and modulus of dowel support values

Dowel Bar	Average k , psi	Average K_o , pci
1.5"ϕ Epoxy-Coated	2,355,618	1,570,173
1.5"ϕ Stainless Steel	1,902,121	1,271,193
1.5"ϕ GFRP	2,265,352	1,512,026
1.875"ϕ GFRP	875,577	467,336

Table 4.14 **Unaged, 1 Million Cycles** - Average modulus of foundation and modulus of dowel support values

Dowel Bar	Average k , psi	Average K_o , pci
1.5"ϕ Stainless Steel	4,315,290	2,885,501
Elliptical GFRP	3,672,690	1,647,085
Shaved GFRP	2,881,515	1,545,786
1.5"ϕ GFRP	1,305,781	870,874
1.875"ϕ GFRP	979,741	523,052

Table 4.15 **Aged, 1 Million Cycles** - Average modulus of foundation and modulus of dowel support values

Dowel Bar	Average k , pci	Average K_o , pci
1.5"ϕ Epoxy-Coated	969,462	646,154
1.5"ϕ Stainless Steel	1,628,247	1,086,978
1.5"ϕ GFRP	1,735,170	1,157,819
1.875"ϕ GFRP	550,633	293,688

Using the data in the tables above and the procedure outlined in Section 4.2.1 the associated bearing stresses can be found. Tables 4.16 thru 4.19 display the calculated results for the Timoshenko and Friberg bearing stresses. Tables 4.16 and 4.17 contain the results for the dowel bars with zero cycles and Tables 4.18 and 4.19 show the results of the dowel bars with one million cycles. Tables 4.16 and 4.18 list the results for unaged specimen while the other two tables show the results for aged specimens.

Table 4.16 **Unaged, 0 Cycles** - Average bearing stress values

Dowel Bar	**Average σ_{bT}, pli**	**Average σ_{bF}, psi**
1.5"ϕ Stainless Steel	2,503	1,673
Elliptical GFRP	3,149	1,410
Shaved GFRP	3,430	1,840
1.5"ϕ GFRP	2,943	1,963
1.875"ϕ GFRP	2,071	1,106

Table 4.17 **Aged, 0 Cycles** - Average bearing stress values

Dowel Bar	**Average σ_{bT}, pli**	**Average σ_{bF}, psi**
1.5"ϕ Epoxy-Coated	2,207	1,472
1.5"ϕ Stainless Steel	2,108	1,408
1.5"ϕ GFRP	3,459	2,309
1.875"ϕ GFRP	1,997	1,066

Table 4.18 **Unaged, 1 Million Cycles** - Average bearing stress values

Dowel Bar	**Average σ_{bT}, pli**	**Average σ_{bF}, psi**
1.5"ϕ Stainless Steel	2,598	1,737
Elliptical GFRP	3,357	1,505
Shaved GFRP	3,423	1,837
1.5"ϕ GFRP	3,001	2,002
1.875"ϕ GFRP	2,055	1,097

Table 4.19 **Aged, 1 Million Cycles** - Average bearing stress values

Dowel Bar	Average σ_{bT}, pli	Average σ_{bF}, psi
1.5"ϕ Epoxy-Coated	1,760	1,173
1.5"ϕ Stainless Steel	2,026	1,353
1.5"ϕ GFRP	3,229	2,155
1.875"ϕ GFRP	1,774	946

When reviewing the bearing stresses from the elemental fatigue results, a few trends can be seen. One trend is apparent when comparing the zero cycle dowel bars to the million cycle dowel bars. In general, the million cycle dowel bars tend to have slightly higher bearing stresses, although, the stresses are very similar in all cases. With the small deflections that are used in the analysis of this data, a safe assumption would be to consider the bearing stresses between the different cycles approximately equal. Another trend is that the Timoshenko bearing stresses are larger than the Friberg bearing stresses. A trend that was also seen with the Iosipescu and AASHTO specimens was that the larger bars of the same material had lower bearing stresses than the smaller dowel bars. This trend is also true with the fatigue testing, with the exception of the Timoshenko bearing stresses with the GFRP alternatively shaped dowel bars. The alternatively shaped dowel bars would have a larger cross-section, but the Timoshenko bearing stresses are significantly higher than smaller GFRP bars. The Friberg bearing stresses do not follow the same trend with the alternatively shaped GFRP dowel bars as the Timoshenko bearing stresses. With the alternatively shaped GFRP dowel bars, the Friberg bearing stress decreases as the Timoshenko bearing stress increases when compared with the other bars. This trend may indicate that the Friberg bearing stresses are underestimated as the dowel bar width increases.

This trend may also indicate that the material removed to create the alternatively shaped GFRP dowels bars is detrimental to the stiffness.

4.3 American Highway Technology Results

The following sections will detail the experimental data that was calculated for the AHT project.

4.3.1 General

The AHT testing method compared round and elliptical steel dowel bars. In this research the round dowel bars were epoxy coated, while the elliptical dowel bars were plain steel with no epoxy coating. The lack of epoxy coating had no effect on the accuracy of the testing since these dowels were not exposed to weather and were tested soon after being cast. This difference in coatings is one reason why aged dowel bars could not be tested on this project.

4.3.2 Elemental Direct Shear Test Method

The purpose of this research was to determine the effect that dowel bar shape and size has on bearing stress at the face of the joint. This test method was outlined in Section 3.2.4. Using the analysis procedure outlined in Section 4.2.1, the following results were obtained. The average relative deflection, shear deflection, and average deflection at the face of the joint are shown in Table 4.20.

Table 4.21 is a listing of each specimen type and the associated average modulus of foundation and modulus of dowel support calculated at a load of 2000 pounds. While Table 4.22 indicates the calculated results for the Timoshenko and Friberg bearing stresses.

Table 4.20 **Direct Shear Method** - Average relative, shear, and face of the joint deflections

Dowel Bar	Average Δ, in.*	Average δ, in.*	Average y_o, in.*
1.5"ϕ Epoxy-Coated	0.001642	0.000014	0.000814
1.25"ϕ Epoxy-Coated	0.002642	0.000020	0.001311
Large Elliptical Steel	0.001968	0.000012	0.000978
Medium Elliptical Steel	0.002432	0.000017	0.001207
Small Elliptical Steel	0.002383	0.000025	0.001179

*Note: The deflections cannot be measured this accurately, but are needed to display the effects of shear deflection.

Table 4.21 **Direct Shear Method** - Average modulus of foundation and modulus of dowel support

Dowel Bar Description	Average k , (psi)	Average K_o, (pci)
1.5"ϕ Epoxy-Coated	2,845,586	1,897,832
1.25"ϕ Epoxy-Coated	1,931,043	1,556,660
Large Elliptical Steel	2,272,200	1,148,216
Medium Elliptical Steel	2,171,172	1,311,940
Small Elliptical Steel	3,088,499	2,195,109

Table 4.22 **Direct Shear Method** - Average bearing stress values

Dowel Bar Description	Average σ_{bT} , (pli)	Average σ_{bF} , (psi)
1.5"ϕ Epoxy-Coated	2,316	1,545
1.25"ϕ Epoxy-Coated	2,532	2,040
Large Elliptical Steel	2,222	1,123
Medium Elliptical Steel	2,621	1,584
Small Elliptical Steel	3,641	2,588

With the Direct Shear Method, the Timoshenko bearing stresses were always larger than the Friberg bearing stresses. This behavior is just as was indicated in all the other test methods. The steel alternatively shaped dowel bars with the Direct Shear Method results indicate that the Timoshenko and Friberg bearing stresses behave in the same manner as the round shapes tested. The behavior of the GFRP alternatively shaped dowel bars used in the Elemental Fatigue test displayed the opposite behavior. The results shown by the steel alternatively shaped dowel bars suggests that the results seen with the alternatively shaped

GFRP bars is caused by the loss in stiffness. However, comparing the bearing stresses of the steel alternatively shaped dowel bars with the round dowel bars still indicates the possibility for an underestimation by Friberg's bearing stress theory.

5.0 THEORETICAL INVESTIGATION

5.1 Introduction

As was discussed in Chapter 2, the relative deflection across a pavement joint is dependent on four separate components. Previous research at ISU neglected two of the deflection terms due to the assumed small values. The terms neglected in previous research was the deflection due to the slope of the dowel bar and flexural deflection.

The equation used to determine the relative deflection across a pavement joint was shown in Chapter 2 and is repeated here for convenience.

$$\Delta = 2y_o + z\left(\frac{dy_o}{dx}\right) + \delta + \frac{Pz^3}{12EI} \tag{2.8}$$

where,

y_o = deflection at the face of the joint (in.)
$\delta = \frac{\lambda Pz}{AG}$, shear deflection (in.) (2.9)
P = load transferred by dowel bar (pounds)
λ = form factor
A = cross-sectional area of the dowel bar ($in.^2$)
G = shear modulus (psi)

As stated above, the terms of interest in this chapter are the deflection due to the slope of the dowel bar, $z\left(\frac{dy_o}{dx}\right)$, and the flexural deflection, $\frac{Pz^3}{12EI}$. As can be seen, both terms neglected contain the joint width, z. The small joint width, z, used in research at ISU was the basis for neglecting the two terms listed above. This chapter will investigate the derivations of each of the terms above, the appropriateness of neglecting these terms, and when including the above terms becomes appropriate in the analysis of k and K_o.

5.2 Dowel Bar Slope Theory

5.2.1 Purpose

The deflection due to the slope of the dowel bar (slope deflection) consists of two separate elements. The first element is the joint width, z, the second element is the slope of the dowel bar at the face of the joint, $\left(\frac{dy_o}{dx}\right)$. The joint width is easy to deal with since this width is a finite value that can easily be measured. On the other hand, the slope of the dowel bar across the face of the joint is a theoretical value and is more difficult to determine. The slope of the dowel bar across a joint was found by work done by Timoshenko and later modified upon by Friberg. Their derivation was completed as follows.

5.2.2 Dowel Bar Slope Derivation

The initial portion of the derivation for dowel bar slope was shown in Chapter 2. This portion will also be repeated here for convenience. Timoshenko found the deflection of a beam on an elastic foundation to be equal to Equation 2.1.

$$EI\frac{d^4y}{dx^4} = -ky \qquad (2.1)$$

where k is a constant (psi), E is the modulus of elasticity of the dowel (psi), I is the moment of inertia of the dowel ($in.^4$), and y is the deflection. Timoshenko indicates that the general solution to this equation is Equation 2.2.

$$y_o = e^{\beta x}(A\cos\beta x + B\sin\beta x) + e^{-\beta x}(C\cos\beta x + D\sin\beta x) \qquad (2.2)$$

where,

$$\beta = \sqrt[4]{\frac{k}{4EI}} = \text{relative stiffness of the beam on the elastic foundation } (in.^{-1}) \qquad (2.3)$$

k = modulus of foundation (psi)

By applying the appropriate boundary conditions, A, B, C and D can be determined. Assume a semi-infinite beam on an elastic foundation with moment, M_0, and a point load P, as shown in Figure 5.1. Solving Equation 2.3 becomes Equation 2.4.

$$y = \frac{e^{-\beta x}}{2\beta^3 EI}[P\cos\beta x - \beta M_o(\cos\beta x - \sin\beta x)] \qquad (2.4)$$

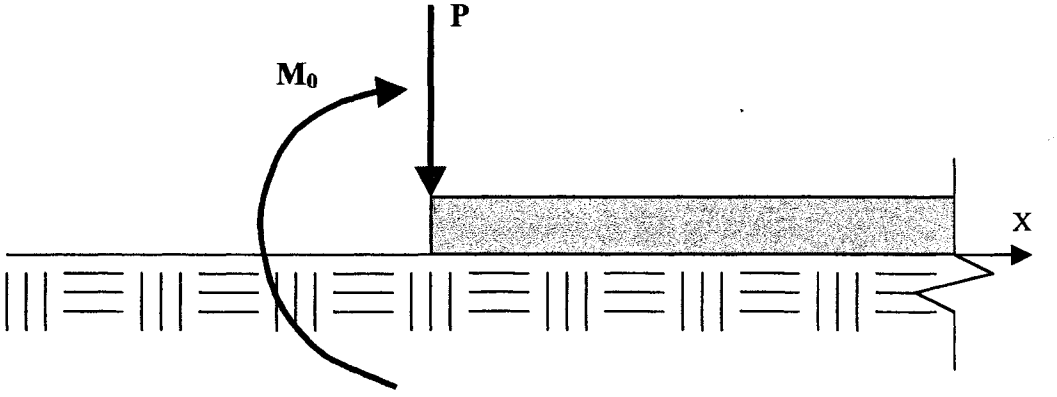

Figure 5.1 Semi-infinite beam on an elastic foundation

The slope of the beam can be determined by differentiating Equation 2.4 with respect to x. This differentiation will determine the slope of the beam at any point along the axis and is shown in Equation 2.5.

$$\frac{dy}{dx} = \frac{e^{-\beta x}}{2\beta^2 EI}[(2\beta M_o - P)\cos\beta x - P\sin\beta x] \qquad (2.5)$$

Friberg applied Timoshenko's elastic beam theory of a semi-infinite beam. Friberg assumed that the inflection point of the dowel occurred in the center of the joint width. Applying this assumption, the forces on the dowel bar are shown in Figure 5.2. Substituting $M_0 = -Pz/2$ and setting x equal to zero Equation 2.4 can be written as Equation 2.6. Equation 2.6 is the deflection of the dowel at the face of the joint, y_o.

$$y_o = \frac{P}{4\beta^3 EI}(2 + \beta z) \tag{2.6}$$

where,

$\beta = \sqrt[4]{\frac{K_o b}{4EI}}$ = relative stiffness of the dowel bar encased in concrete ($in.^{-1}$) (2.7)

K_o = modulus of dowel support (pci)
b = dowel bar width (in.)
E = modulus of elasticity of the dowel bar (psi)
I = moment of inertia of the dowel bar ($in.^4$)
P = load transferred through the dowel bar (pounds)
z = joint width (in.)

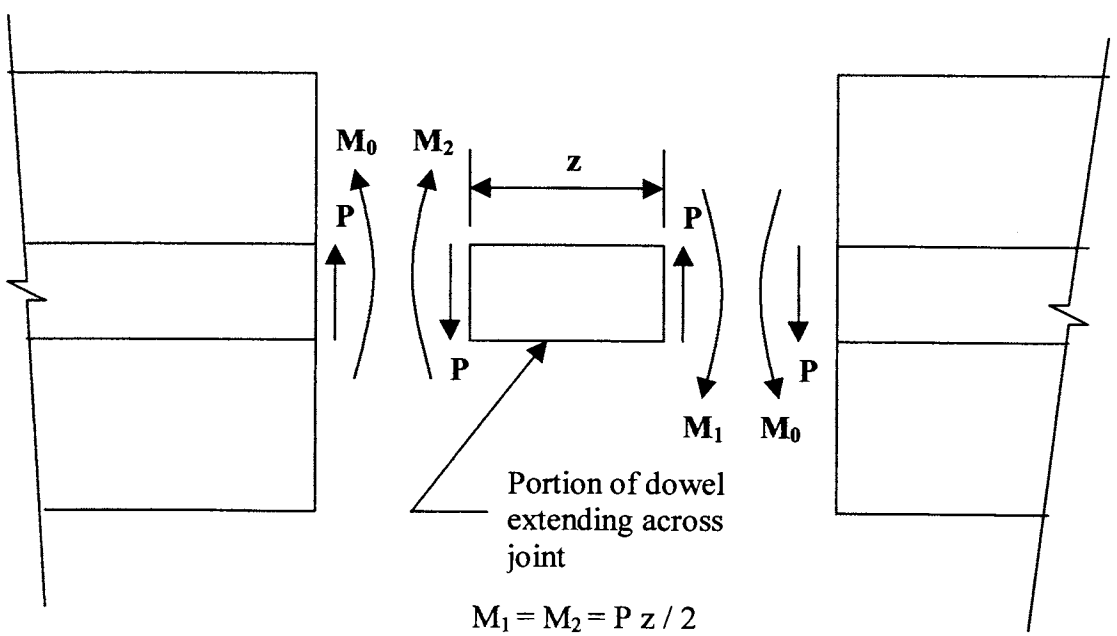

$M_1 = M_2 = P\,z / 2$

$M_0 = -M_1 = -M_2 = -P\,z / 2$

Figure 5.2 Forces acting on a dowel bar

The slope of the dowel at the face of the joint can be found in a similar manner to the deflection, y_o. Again, substituting $M_0 = -Pz/2$ and setting x equal to zero into Equation 2.5

will yield the slope at the face of the joint. Equation 5.1 shows the slope of the dowel at the face of the joint.

$$\frac{dy_o}{dx} = \frac{-P}{2\beta^2 EI}(1+\beta z) \tag{5.1}$$

5.2.3 Slope Deflection and K_o

As was shown in Chapter 3, the relative deflection across a joint, y_o, can be determined without calculating the slope deflection. Previous research at ISU neglected the slope deflection due to the assumed effect over a small joint width, z. When the slope deflection is used to calculate the solution of K_o, a similar method is utilized as in Chapter 3. The remainder of this section will show the proper method used to determine K_o, and the concrete bearing stress, σ_b, when including slope deflection in the calculation.

The relative deflection across a pavement joint, Δ, was shown in Equation 2.8. Neglecting flexural deflection Equation 2.8 can be rewritten as Equation 5.2.

$$\Delta = 2y_o + z\left(\frac{dy_o}{dx}\right) + \delta \tag{5.2}$$

The deflection at the face of the joint, y_o, and the slope deflection are both dependant on K_o. The relative deflection across the joint, Δ, is determined from lab experiments. The shear deflection, δ, can easily be computed from the properties of the dowel bar. Reorganizing Equation 5.2 by placing the terms that are dependent on K_o on the same side of the equation; Equation 5.3 can be determined.

$$\Delta - \delta = 2y_o + z\left(\frac{dy_o}{dx}\right) \tag{5.3}$$

Substituting various values of K_o into Equations 2.6 and 5.1 a graph can be created showing the right side of Equation 5.3 versus K_o. Figure 5.3 shows a graphical illustration for a 1.5-in. diameter epoxy-coated steel dowel bar at a 2000-pound load.

The next step in determining K_o is to evaluate the terms on the left side of Equation 5.3. Using experimental data, a value can be calculated for the left side of Equation 5.3. Once this value is known, a chart similar to that shown Figure 5.3 is used to determine the K_o value.

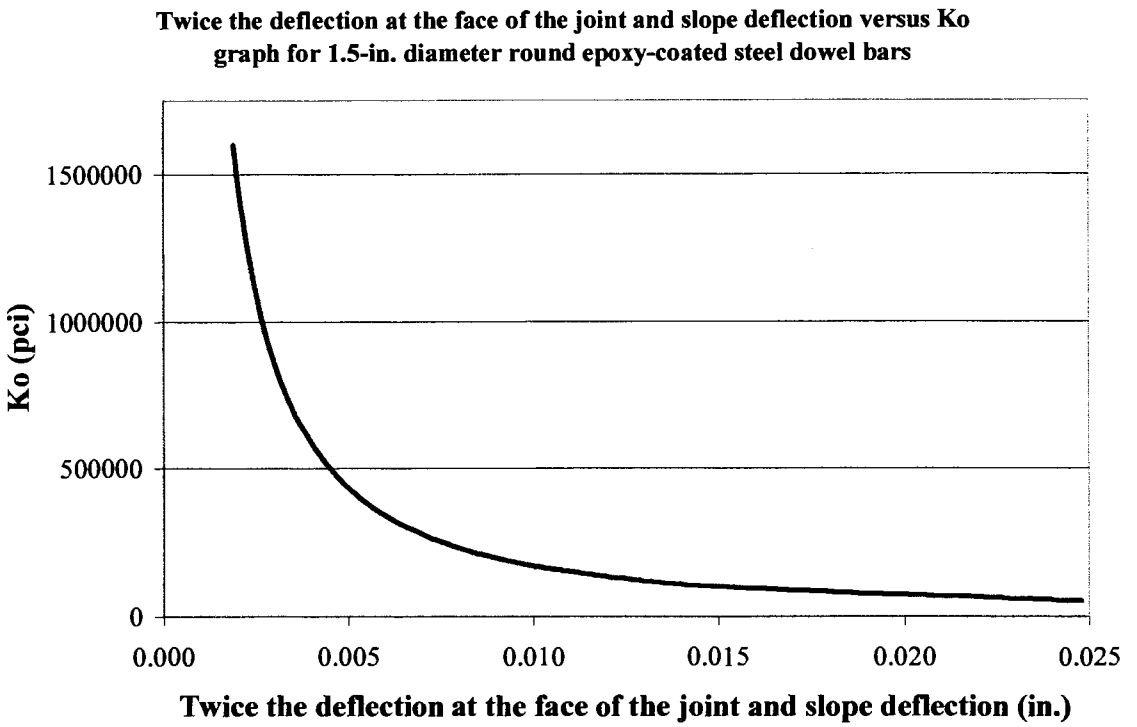

Figure 5.3 Twice the deflection at the face of the joint, $2*y_o$, and slope deflection versus K_o

Once the K_o value is known, the whole previous procedure is used to determine a value for the deflection at the face of the joint, y_o. Substituting various values of K_o into Equation 2.6, a graph can be created showing K_o versus deflection at the face of a joint, y_o.

Figure 5.4 shows a K_o versus y_o graph for a 1.5-in. diameter epoxy-coated steel dowel bar at a 2000-pound load. Once K_o and y_o have been determined, all pertinent values can easily be determined using simple mathematics. The results of this section will be shown in the following chapter.

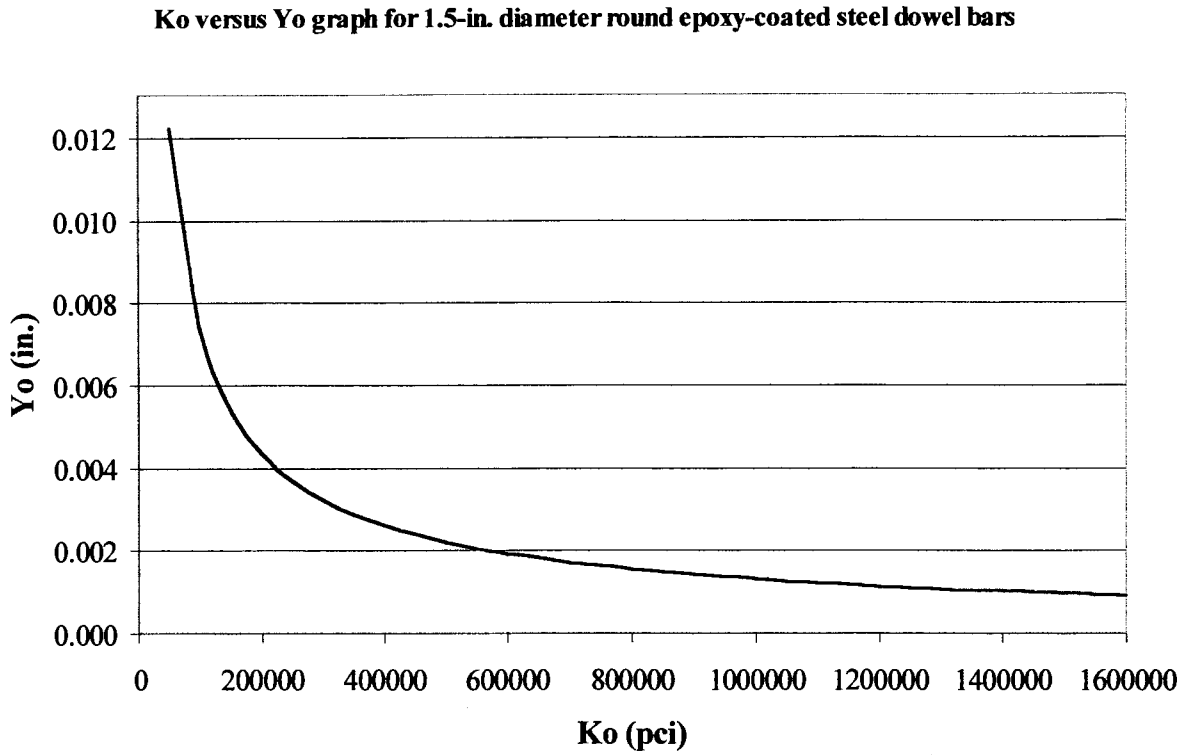

Figure 5.4 K_o versus y_o for the 1.5-in. diameter round epoxy-coated steel dowel Bar

5.3 Flexural Deflection Theory

5.3.1 Purpose

As was discussed in Section 5.1, the flexural deflection term was neglected from Equation 2.8 when calculating K_o in previous research done at ISU. The flexural deflection,

$\frac{Pz^3}{12EI}$, is simple to evaluate, but was neglected due to the small joint width used in research at ISU. In the following section a derivation of the flexural deflection term is completed.

5.3.2 Flexural Deflection Derivation

The dowel bar pavement system can easily be analyzed as a beam that is fixed on one end with a load applied on the opposite end. The opposite end is free to translate vertically but is restrained from rotating. Figure 5.5 shows the idealized beam for a dowel bar spanning across a pavement joint of width z. Figure 5.6 shows the shear diagram and moment diagram for the idealized beam.

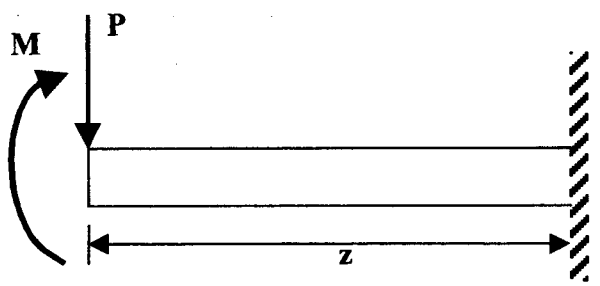

$$M = P\,z / 2$$

Figure 5.5 Idealized beam of dowel bar

From engineering mechanics, the relationship between shear, moment, slope and deflection are known. These relationships will be used to derive the flexural deflection. The shear is constant along the entire length of the beam, therefore the shear equation is a constant. The shear can be determined at any place on the beam using Equation 5.4.

$$V(x) = -P \tag{5.4}$$

The moment is simply the integral of the slope, which is shown in Equation 5.5.

$$M(x) = \int V(x)dx = -Px + Y \tag{5.5}$$

Y is a constant that can be solved using the known boundary conditions for the beam. In this case the moment at x = z is equal to $\frac{-Pz}{2}$. Solving for Y, Equation 5.5 can be rewritten as Equation 5.6.

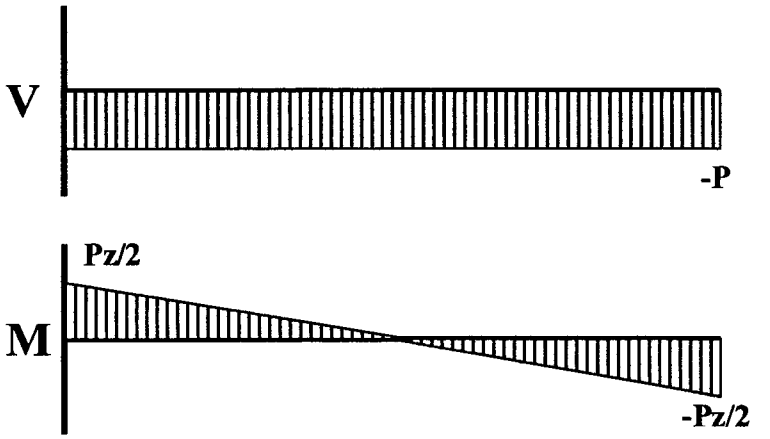

Figure 5.6 Shear and moment diagrams for idealized beam of dowel bar

$$M(x) = -Px + \frac{Pz}{2} \tag{5.6}$$

The method above can be repeated to determine the flexural slope and the flexural deflection of the dowel bar. Deviations for the flexural slope and flexural deflection are shown in Equations 5.7 and 5.8, respectively.

$$\theta(x) = \frac{1}{EI}\int M(x)\,dx = \frac{-Px^2 + Pzx}{2EI} \tag{5.7}$$

$$\Delta(x) = \int\theta(x)dx = \frac{-2Px^3 + 3Pzx^2 - Pz^3}{12EI} \tag{5.8}$$

5.3.3 Flexural Deflection and K_o

Determining K_o including flexural deflection in the equation is a simple process. Since flexural deflection contains no K_o term, the flexural deflection value can simply be added into the equation and the K_o value determined. Including slope deflection in the determination of K_o does not change the process used to calculate flexural deflection. Essentially, flexural deflection is simply a value that is added to the equation, but does not change the method used to determine K_o. The flexural deflection results will be shown in Chapter 6.

6.0 ANALYSIS OF THEORETICAL RESULTS

6.1 Introduction

The theoretical explanations of two previously neglected deflection terms were discussed in Chapter 5. The derivation of these terms was shown and the proper method used to calculate the new modulus of dowel support, K_o, was also shown. This chapter will show the effects that these two deflection terms have on K_o and the bearing stress of the concrete dowel bar interface. The results will also be discussed and the effects analyzed. A load of 2000 pounds was used to calculate all the values shown throughout this chapter.

6.2 Slope Deflection Results

Using the method outlined in Section 5.2.3, the influence of slope deflection on experimental results of the modulus of dowel support and the concrete bearing stress can be determined. The remainder of this section will compare the effect that slope deflection has on the modulus of dowel support, the deflection at the face of the joint, the bearing stress and other effects.

6.2.1 Iowa Department of Transportation Results

The following section will compare the experimental data from the IDOT project with the slope deflection modified values.

6.2.1.1 Iosipescu Test Method & AASHTO Shear Test Method

Table 6.1 is a listing of each unaged specimen type and the associated average modulus of dowel support, K_o, the average slope deflection adjusted modulus of dowel support, K_{oSD}, and the amount of error that was introduced when neglecting the slope deflection term. Table 6.2 shows the aged specimens values for the average modulus of

dowel support, K_o, the average slope deflection adjusted modulus of dowel support, K_{oSD}, and the amount of error that was introduced when neglecting the slope deflection term.

Table 6.1 **Unaged** - Average modulus of dowel support, slope deflection adjusted modulus of dowel support, and associated error neglecting slope deflection

Dowel Bar	Average K_o, pci	Average K_{oSD}, pci	Error, %
Iosipescu			
1.5"ϕ Epoxy-Coated	772,330	803,524	-4.04
1.5"ϕ Stainless Steel	665,170	690,817	-3.86
1.5"ϕ Plain Steel	976,750	1,018,187	-4.24
1.5"ϕ GFRP	598,443	634,866	-6.09
1.75"ϕ GFRP	300,000	312,513	-4.17
Modified AASHTO			
1.5"ϕ Epoxy-Coated	377,774	390,702	-3.42
1.5"ϕ Aluminum	251,133	261,269	-4.04
1.957"ϕ Aluminum	176,500	181,755	-2.98
1.5"ϕ Copper	355,786	369,594	-3.88
1.714"ϕ Copper	332,032	343,242	-3.38
1.5"ϕ GFRP	299,847	315,217	-5.13
1.875"ϕ GFRP	256,233	266,427	-3.98

Table 6.2 Iosipescu Test - **Aged** - Average modulus of dowel support, slope deflection adjusted modulus of dowel support, and associated error neglecting slope deflection

Dowel Bar	Average K_o, pci	Average K_{oSD}, pci	Error, %
1.5"ϕ Epoxy-Coated	704,950	732,866	-3.96
1.5"ϕ Stainless Steel	861,930	897,097	-4.08
1.5"ϕ Plain Steel	954,071	994,352	-4.22
1.5"ϕ GFRP	740,432	787,701	-6.38
1.875"ϕ GFRP	303,404	316,030	-4.16

As shown above in Tables 6.1 and 6.2, the average modulus of dowel support, K_o, is underestimated in every instance when the slope deflection was neglected. The error ranges from 2.98% to 6.38%. In general, the stiffer the dowel bar, the smaller the error introduced in neglecting the slope deflection. Table 6.3 shows the error introduced on the modulus of dowel support when neglecting slope deflection compared to the stiffness, EI, of each type of dowel bar. Table 6.3 is arranged with the stiffest dowel bars first with more flexible dowel bars last.

Table 6.3 Dowel material, size, stiffness, and K_o slope deflection error

Material	Diameter, in.	EI, (10^6) lb-in.^{2}	Error, %
Epoxy-Coated Steel	1.5	7.206	-3.81
Plain Steel	1.5	7.206	-4.23
Copper	1.714	7.202	-3.38
Aluminum	1.957	7.200	-2.98
Stainless Steel	1.5	6.958	-3.97
Copper	1.5	4.225	-3.88
GFRP	1.875	3.950	-4.07
GFRP	1.75	2.854	-4.17
Aluminum	1.5	2.485	-4.04
GFRP	1.5	1.225	-5.87

Table 6.3 indicates that, in general, the error of K_o increases as the stiffness of the dowel bar decreases. This behavior would be appropriate since a stiffer bar would have less overall deflection, which would result in less sloping of the dowel bar. Less sloping of the dowel bar across the joint would result in less deflection due to slope. Furthermore, consider that, in general, stiffer bars would have a higher K_o value than dowel bars with a lower stiffness. When a larger K_o value is combined with a smaller overall slope deflection, a smaller slope deflection error would be expected.

Table 6.4 shows each unaged specimen type and associated average deflection at the face of the joint, y_o, the average slope deflection adjusted deflection at the face of the joint, y_{oSD}, and the amount of error that was introduced when neglecting the slope deflection term. Similarly, Table 6.5 lists each aged specimen type and associated average deflection at the face of the joint, y_o, the average slope deflection adjusted deflection at the face of the joint, y_{oSD}, and the amount of error that was introduced when neglecting slope deflection.

Table 6.4 **Unaged** - Average deflection at the face of the joint, slope deflection adjusted deflection at the face of the joint, and associated error neglecting slope deflection

Dowel Bar	Average y_o, in.*	Average y_{oSD}, in.*	Error, %
Iosipescu			
1.5"ϕ Epoxy-Coated	0.001589	0.001543	2.90
1.5"ϕ Stainless Steel	0.001793	0.001744	2.78
1.5"ϕ Plain Steel	0.001334	0.001294	3.04
1.5"ϕ GFRP	0.003035	0.002905	4.28
1.75"ϕ GFRP	0.003634	0.003526	2.99
Modified AASHTO			
1.5"ϕ Epoxy-Coated	0.002706	0.002639	2.47
1.5"ϕ Aluminum	0.004815	0.004675	2.90
1.957"ϕ Aluminum	0.003909	0.003825	2.16
1.5"ϕ Copper	0.003244	0.003153	2.79
1.714"ϕ Copper	0.002698	0.002632	2.44
1.5"ϕ GFRP	0.005065	0.004881	3.64
1.875"ϕ GFRP	0.003565	0.003463	2.86

*Note: The deflections cannot be measured this accurately, but are needed to show the effects of slope deflection.

Unlike the modulus of dowel support, neglecting the slope deflection overestimates the deflection at the face of the joint. This trend seems appropriate since a term was ignored

Table 6.5 Iosipescu Test - **Aged** - Average deflection at the face of the joint, slope deflection adjusted deflection at the face of the joint, and associated error neglecting slope deflection

Dowel Bar	Average y_o, in.*	Average y_{oSD}, in.*	Error, %
1.5"ϕ Epoxy-Coated	0.001701	0.001653	2.85
1.5"ϕ Stainless Steel	0.001479	0.001436	2.93
1.5"ϕ Plain Steel	0.001358	0.001317	3.03
1.5"ϕ GFRP	0.002592	0.002476	4.48
1.875"ϕ GFRP	0.003144	0.003050	2.98

*Note: The deflections cannot be measured this accurately, but are needed to show the effects of shear deflection.

in the equation. The total relative deflection is a known value that is developed through experimentation. The relative deflection is equal to the deflection at the face of the joint along with the shear deflection and possibly other terms as shown in Equation 2.8. If one term is ignored than the portion of the deflection that was associated with the ignored term gets incorrectly attributed to the remaining terms. This behavior explains why the deflection at the face of the joint decreases when slope deflection is considered.

Another trend that can be seen in Tables 6.4 and 6.5 is that the error in neglecting the deflection at the face of the joint is lower for the stiffer dowel bars. This is the same trend that was seen with the error for the modulus of dowel support. Table 6.6 shows the error introduced on the deflection at the face of the joint when neglecting slope deflection compared to the stiffness, EI, of each type of dowel bar. Table 6.6 is arranged with decreasing stiffness of the dowel bars.

As in Table 6.3, there seems to be a trend that shows the higher the stiffness of the dowel bar the lower the error introduced into the deflection at the face of the joint. As discussed above, the deflection at the face of the joint decreased when slope deflection was

considered. This trend is due to the fact that the actual slope deflection used in the calculation was incorrectly attributed to the deflection at the face of the joint when slope deflection was neglected, as explained previously. Since this error introduced into the deflection at the face of the joint is directly related to the magnitude of slope deflection the trend holds that a stiffer dowel bar would develop less slope under load. If the dowel bar will slope less, than there will obviously be less deflection due to the slope of the dowel bar.

Table 6.6 Dowel bar material, size, stiffness, and y_o slope deflection error

Material	Diameter, in.	EI, (10^6) lb-in.^{2}	Error, %
Epoxy-Coated Steel	1.5	7.206	2.74
Plain Steel	1.5	7.206	3.04
Copper	1.714	7.202	2.44
Aluminum	1.957	7.200	2.16
Stainless Steel	1.5	6.958	2.86
Copper	1.5	4.225	2.79
GFRP	1.875	3.950	2.92
GFRP	1.75	2.854	2.99
Aluminum	1.5	2.485	2.90
GFRP	1.5	1.225	4.13

The last area that needs to be reviewed is the bearing stress at the dowel bar concrete interface. As was stated in Section 4.2.1, the bearing stress is simply the modulus of dowel support multiplied by the deflection at the face of the joint. In this instance, multiply the slope deflection adjusted modulus of dowel support, K_{oSD}, times the slope deflection adjusted deflection at the face of the joint, y_{oSD}. This product equals the slope deflection adjusted bearing stress and is shown in Equation 6.1.

$$\sigma_{bSD} = K_{oSD} * y_{oSD} \tag{6.1}$$

Table 6.7 shows the average Friberg bearing stress, the average slope deflection adjusted bearing stress and the percent error due to neglecting the slope deflection for the unaged specimens. Similarly, Table 6.8 shows the average Friberg bearing stress, the average slope deflection adjusted bearing stress, and the associated error due to neglecting the slope deflection for the aged specimens.

Table 6.7 **Unaged** - Average Friberg bearing stress, slope deflection adjusted bearing stress, and associated error neglecting slope deflection

Dowel Bar	Average σ_b, psi	Average σ_{bSD}, psi	Error, %
Iosipescu			
1.5"ϕ Epoxy-Coated	1227	1240	-1.02
1.5"ϕ Stainless Steel	1193	1205	-0.97
1.5"ϕ Plain Steel	1303	1317	-1.07
1.5"ϕ GFRP	1816	1844	-1.54
1.75"ϕ GFRP	1090	1102	-1.06
Modified AASHTO			
1.5"ϕ Epoxy-Coated	1022	1031	-0.86
1.5"ϕ Aluminum	1209	1222	-1.02
1.957"ϕ Aluminum	690	695	-0.75
1.5"ϕ Copper	1154	1166	-0.98
1.714"ϕ Copper	896	903	-0.85
1.5"ϕ GFRP	1519	1539	-1.30
1.875"ϕ GFRP	913	923	-1.01

A difference in bearing stress was expected due to a change seen in both the modulus of dowel support and the deflection at the face of the joint. However, due to the opposite effects on each term, the significance of the bearing stress error was unknown until the actual values had been calculated. As was shown in Tables 6.7 and 6.8, neglecting the slope deflection underestimates the bearing stress of the dowel bar-concrete interface for all dowel

Table 6.8 Iosipescu Test - **Aged** Average Friberg bearing stress, slope deflection adjusted bearing stress, and associated error neglecting slope deflection

Dowel Bar	Average σ_b, psi	Average σ_{bSD}, psi	Error, %
1.5"ϕ Epoxy-Coated	1199	1211	-1.00
1.5"ϕ Stainless Steel	1275	1288	-1.03
1.5"ϕ Plain Steel	1296	1309	-1.06
1.5"ϕ GFRP	1919	1950	-1.62
1.875"ϕ GFRP	954	964	-1.05

bar types. The bearing stress is consistently underestimated by approximately 1% for each type of dowel bar.

6.2.1.2 Elemental Fatigue Test Method

As was discussed in Section 4.2.2, this method of testing was intended to determine the relative amount of oblonging of the hole for different types of dowel bars. The concern of this thesis is the effect that slope deflection has on the areas previously tested at ISU. Therefore, the results from this test method will be used to compare the effects of slope deflections and oblonging.

The effect of slope deflection on oblonging can be explained in simple terms. The value of significance in regard to oblonging around the dowel bar is the difference between the zero cycle modulus of dowel support and the million-cycle modulus of dowel support. The effect of slope deflection on the modulus of dowel support was shown in the previous tables in this chapter. While the effect of slope deflection will change the value of the modulus of dowel support, this change will be maintained for each value. Therefore, each modulus of dowel support value will be altered by a similar value. While the difference between these values will not be identical, the relative amount will be similar and the relationship between values maintained when slope deflection is included.

To illustrate the previous discussion, the aged specimens are shown in Tables 6.9 and 6.10. Table 6.9 shows the average modulus of dowel support, K_o, for zero cycles and one million cycles, as well as the percentage difference between the two modulii. Table 6.10 will incorporate the slope deflection and show the average slope deflection adjusted modulus of dowel support, K_{oSD}, for zero cycles and one million cycles, as well as the percentage difference between the two modulii.

Table 6.9 **Aged** - Average modulus of dowel support at zero cycles, average modulus of dowel support at one million cycles, percentage difference

Dowel Bar	**Zero Cycles**	**One Million Cycles**	**Difference , %**
	Average K_o , pci		
1.5"ϕ Epoxy-	1,570,173	646,154	41.69
1.5"ϕ Stainless	1,271,193	1,086,978	7.81
1.5"ϕ GFRP	1,512,026	1,157,819	13.27
1.875"ϕ GFRP	467,336	293,688	22.82

Table 6.10 **Aged** - Average slope adjusted modulus of dowel support at zero cycles, average slope adjusted modulus of dowel support at one million cycles, percentage difference

Dowel Bar	**Zero Cycles**	**One Million Cycles**	**Difference , %**
	Average K_{oSD} , pci		
1.5"ϕ Epoxy-	1,643,260	671,255	42.00
1.5"ϕ	1,327,427	1,133,516	7.88
1.5"ϕ GFRP	1,623,735	1,239,000	13.44
1.875"ϕ GFRP	488,977	305,806	23.05

As illustrated in Tables 6.9 and 6.10, the percentage difference of the modulus of dowel support over extended cycles when neglecting slope deflection is nearly identical as to the percentage difference when considering slope deflection. Although the values of the

modulus of dowel support and bearing stress vary when including slope deflection, the effects to the relationships between the values remains the same.

6.2.2 American Highway Technology Results

The following section will compare the experimental values of the AHT project to the slope deflection modified values. As discussed in Section 4.3, the elemental direct shear method was used to evaluate five different steel dowel bars. The AHT project was designed to compare the modulus of dowel support and bearing stress for round dowel bars and different sizes of steel elliptical dowel bars. In this section the effect of neglecting slope deflection will be evaluated to determine if elliptical dowel bars are effected the same as round dowel bars.

Table 6.11 shows each specimen type and the associated average modulus of dowel support, K_o, the average slope deflection adjusted modulus of dowel support, K_{oSD}, and the amount of error that was introduced when neglecting slope deflection.

Table 6.11 – **Direct Shear Method** - Average modulus of dowel support, slope deflection adjusted modulus of dowel support, and associated error neglecting slope deflection

Dowel Bar	Average K_o, pci	Average K_{oSD}, pci	Error, %
Round			
1.5"ϕ Epoxy-Coated	1,897,832	1,988,508	-4.78
1.25"ϕ Epoxy-Coated	1,556,660	1,629,522	-4.68
Elliptical			
Large Elliptical Steel	1,148,216	1,202,719	-4.75
Medium Elliptical Steel	1,311,940	1,382,681	-5.39
Small Elliptical Steel	2,195,109	2,359,479	-7.49

As can be seen above, the percentage of error introduced by neglecting slope deflection seems to be comparable for round and elliptical steel dowel bars. As the bars get smaller, the amount of error introduced increases. However, one important item about the dowel bars is that the large steel elliptical dowel bar and the 1.5-in. diameter round epoxy-coated steel dowel bar have approximately the same percentage error in neglecting slope deflection. The importance of this distinction is that a large steel elliptical dowel bar requires more total steel than a 1.5-in. diameter epoxy-coated dowel bar. This trend indicates that the 1.5-in. diameter epoxy-coated steel dowel bar may be more resistant to slope deflection and, thereby, stiffer than a similarly sized steel elliptical dowel bar. Having indicated that the round dowel bar is stiffer and less resistant to slope deflection, the overall impact on the modulus of dowel support will be small.

As was shown in Section 6.2.1, the bearing stress is underestimated when neglecting slope deflection effects on the dowel bar system. Table 6.12 compares the error introduced in the bearing stresses when neglecting slope deflection for round and elliptical steel dowel bars.

Table 6.12 – **Direct Shear Method** - Average Friberg bearing stress, slope deflection adjusted bearing stress, and associated error neglecting slope deflection

Dowel Bar	Average σ_b, psi	Average σ_{bSD}, psi	Error, %
Round			
1.5"ϕ Epoxy-Coated	1,545	1,564	-1.24
1.25"ϕ Epoxy-Coated	2,040	2,056	-0.75
Elliptical			
Large Elliptical Steel	1,123	1,137	-1.26
Medium Elliptical Steel	1,584	1,606	-1.40
Small Elliptical Steel	2,588	2,638	-1.93

The slope deflection appears to have different effects on the bearing stress for the different types of dowel bars. The elliptical dowel bars seem to be underestimated slightly more as the elliptical dowel bars decrease in size. However, the round dowel bars appear to have the complete opposite behavior. This difference between the types of dowel bars could be attributed to the lack of stiffness due to the shape of the elliptical dowel bars, as was discussed previously. This lower stiffness in the steel elliptical dowel bars could cause a greater increase in slope deflection relative to the round dowel bars deflections across the joint.

The bearing stresses change a greater amount as dowel bar size increases for the steel round dowel bars, while the opposite behavior is noticed with the steel elliptical dowel bars. This difference in behavior suggests that there is a larger increase in all other deflections compared to slope deflection for the steel round dowel bars. Stated another way, the slope deflection has a larger impact on the elliptical dowel bars due to the lower stiffness that was discussed previously.

6.3 Flexural Deflection Results

Using the procedure outlined in Section 5.3.3, the effect of flexural deflection on the experimental results can be determined. The following section will investigate the effects that flexural deflection has on the modulus of dowel support, K_o, the deflection at the face of the joint, y_o, the bearing stress, and other items of interest.

6.3.1 Iowa Department of Transportation Results

The following section will compare the IDOT experimental results with the flexural deflection adjusted results.

6.3.1.1 Iosipescu Test Method & AASHTO Shear Test Method

Table 6.13 compares the unaged specimens average modulus of dowel support, K_o, with the average flexural deflection adjusted modulus of dowel support, K_{oFD}, and the associated error in neglecting the flexural deflection term. Table 6.14 shows the aged specimen average modulus of dowel support, K_o, with the average flexural deflection adjusted modulus of dowel support, K_{oFD}, and the associated error in neglecting the flexural deflection term.

As can readily be seen in Tables 6.13 and 6.14, the effect of the flexural deflection on the modulus of dowel support is negligible. The 1.5-in. diameter GFRP dowel bar shows 0.01% of error introduced by neglecting flexural deflection. In fact, of all the dowel bars tested in this research, the only dowel bars that show 0.01% of error is the 1.5-in. diameter GFRP dowel bar. All of the other dowel bars in the IDOT testing had less than 0.01% error introduced by neglecting the flexural deflection term.

The deflection at the face of the joint, y_o, follows the exact same trend shown in Tables 6.13 and 6.14. The deflection at the face of the joint only has 0.01% error in neglecting flexural deflection in the 1.5-in. diameter GFRP dowel bars. All other dowel bars have less than 0.01% error.

When looking at the bearing stress, none of the dowel bars have any measurable change. Of all the different dowel bars tested in the IDOT research, using the methods outlined above, none of the dowel bars showed any change in the actual bearing stress value, when considering flexural deflection.

Table 6.13 **Unaged** - Average modulus of dowel support, flexural deflection adjusted modulus of dowel support, and associated error neglecting flexural deflection

Dowel Bar	Average K_o, pci	Average K_{oFD}, pci	Error, %
Iosipescu			
1.5"ϕ Epoxy-Coated	772,330	772,345	0.00
1.5"ϕ Stainless Steel	665,170	665,185	0.00
1.5"ϕ Plain Steel	976,750	976,772	0.00
1.5"ϕ GFRP	598,443	598,478	-0.01
1.75"ϕ GFRP	300,000	300,006	0.00
Modified AASHTO			
1.5"ϕ Epoxy-Coated	377,774	377,778	0.00
1.5"ϕ Aluminum	251,133	251,138	0.00
1.957"ϕ Aluminum	176,500	176,501	0.00
1.5"ϕ Copper	355,786	355,792	0.00
1.714"ϕ Copper	332,032	332,036	0.00
1.5"ϕ GFRP	299,847	299,858	0.00
1.875"ϕ GFRP	256,233	256,237	0.00

Table 6.14 Iosipescu Test - **Aged** - Average modulus of dowel support, flexural deflection adjusted modulus of dowel support, and associated error neglecting flexural deflection

Dowel Bar	Average K_o, pci	Average K_{oFD}, pci	Error, %
1.5"ϕ Epoxy-Coated	704,950	704,963	0.00
1.5"ϕ Stainless Steel	861,930	861,948	0.00
1.5"ϕ Plain Steel	954,071	954,042	0.00
1.5"ϕ GFRP	740,432	740,483	-0.01
1.875"ϕ GFRP	303,404	303,409	0.00

6.3.1.2 Elemental Fatigue Test Method

As with the Iosipescu and modified AASHTO testing, the flexural deflection also has little effect on the Elemental Fatigue testing. The modulus of dowel support, K_o, shows 0.01% of error on the 1.5-in. diameter GFRP dowel bars, the elliptical GFRP dowel bars, the

shaved GFRP dowel bars, and the million cycle 1.5-in. diameter stainless steel dowel bars. The other bars contain less than 0.01% error introduced by neglecting flexural deflection.

With the deflection at the face of the joint, y_o, the 1.5-in. diameter stainless steel dowel bar does not have 0.01% error when neglecting the flexural deflection. The 1.5-in. diameter GFRP dowel bar, the elliptical GFRP dowel bar, and the shaved GFRP dowel bars still contain 0.01% error. As with the modulus of dowel support, K_o, the remaining bars also have less than 0.01% error with the deflection at the face of the joint.

The bearing stress is the same as in the Iosipescu and modified AASHTO testing. Considering flexural deflection has no significant effect on bearing stress values. The elliptical GFRP dowel bar at zero cycles is the only dowel bar with any change in the bearing stress value. The value of the bearing stress considering flexural deflection goes up one psi on the elliptical GFRP dowel bar at zero cycles. This small change in bearing stress is not enough to register even a 0.01% change. However, this research is based on a 1/8" joint width. An increase in joint width will cause the flexural deflection to increase at a cubic. Therefore, more research on flexural deflection with larger joint widths is recommended.

6.3.2 American Highway Technology Results

The results indicated above are similar to the results returned in the AHT project. In Section 6.3.1, the results of the research compared the original values to the flexural deflection modified values. In this section, a comparison will be made of the slope deflection modified values to the results obtained when using the slope deflection and flexural deflection modified values.

Table 6.15 shows the slope deflection adjusted modulus of dowel support, K_{oSD}, compared to the slope deflection and flexural deflection adjusted modulus of dowel support, K_{oSDFD} and the associated error due to neglecting flexural deflection.

Table 6.15 – **Direct Shear Method** - Average slope deflection adjusted modulus of dowel support, slope and flexural deflection adjusted modulus of dowel support, and associated error neglecting flexural deflection

Dowel Bar	Average K_{oSD}, pci	Average K_{oSDFD}, pci	Error, %
Round			
1.5"ϕ Epoxy-Coated	1,988,508	1,988,584	0.00
1.25"ϕ Epoxy-Coated	1,629,522	1,629,601	0.00
Elliptical			
Large Elliptical Steel	1,202,719	1,202,759	0.00
Medium Elliptical Steel	1,382,681	1,382,755	0.00
Small Elliptical Steel	2,359,479	2,359,805	0.00

As in Section 6.3.1, the difference introduced into the values is insignificant. The values returned in the AHT research indicate that there was no change introduced even when measured to the one-hundredth of a percent. When comparing the changes made to the associated bearing stresses, there is also no difference. No dowel bar in the AHT research showed any change in bearing stress when considering flexural deflection. Including the effects of flexural deflection is even less significant when slope deflection is included. This trend does follow expectations, because including slope deflection into the equation increases the values of both the modulus of dowel support and the bearing stress.

7.0 SUMMARY, CONCLUSIONS AND RECOMENDATIONS

7.1 Summary

Theoretical calculations were done to compare the effects of slope deflection and flexural deflection on a dowel bar-concrete system. Calculations compared the effects on the modulus of dowel support, the deflection at the face of the joint, and concrete bearing stress. The following section provides a summary of the effects, and later sections provide conclusions and recommendations.

7.1.1 Slope Deflection Summary

The modulus of dowel support showed the largest change when slope deflection was included in the calculation. The addition of slope deflection increased the modulus of dowel support by approximately 3-6%. The addition of slope deflection decreased the deflection at the face of the joint by approximately 3-4%. This decrease in the deflection of the joint seems appropriate considering that another term is added to the equation used to determine the total relative deflection. The total relative deflection is a fixed value for each dowel bar determined through experimentation. The more terms that make up the relative deflection, the less each term would contribute.

The final area measured was the concrete bearing stress. The modulus of dowel support and the deflection at the face of the joint varied more than the bearing stress. The effects on the modulus of dowel support and the deflection at the face of the joint were both in opposite directions; one increased while the other decreased, respectively. Since the modulus of dowel support and the deflection at the face of the joint are directly applied to determine the bearing stress, the result was only an increase of approximately 1% for each dowel bar.

Another trend that was seen in the theoretical analysis is related to the dowel bar stiffness. In general, a stiffer dowel bar had a smaller change in all categories. This trend could especially be seen in smaller GFRP dowel bars. The more work that is done with GFRP dowel bars, the more important considering slope deflection becomes.

One last important consideration that was not tested in this research, is the effect joint width has when determining slope deflection. One variable in the slope deflection term is the joint width, z. The other variable is directly related to slope deflection, which was derived earlier in this paper. Since slope deflection is dependent on the joint width, an increase in joint width will likely cause the slope deflection to increase as well. However, the exact amount of increase in slope deflection cannot be estimated. The effect of joint width can only be determined through experimentation due to the slope deflection terms association with the β variable.

7.1.2 Flexural Deflection Summary

When considering flexural deflection, there was virtually no change in the modulus of dowel support, the deflection at the face at the joint, or the concrete bearing stress. The 1.5-in. diameter GFRP dowel bar had a change of 0.01%, but the other dowel bars showed no change at all. The small change in the GFRP dowel bar, 0.01% change, is so insignificant that experimental data cannot be recorded accurately enough to track this change. The flexural deflection for the experimental results had very little impact.

One final consideration is the effect of joint width on flexural deflection. The flexural deflection term is calculated by cubing the joint width, z. Therefore, any increase in joint width will have a substantial effect on flexural deflection. For example, in this research, a joint width of 1/8 in. was used to replicate a contraction joint. If a 1/2-in. joint width was

used to replicate an expansion joint, the flexural deflection would be 64 times greater than the flexural deflection of the 1/8-in. contraction joint. This example shows what a dramatic effect joint width has on the flexural deflection term.

7.2 Conclusions

The relationships outlined throughout this research, in regards to the effects of slope deflection and flexural deflection, may best be shown in the following table. Table 7.1 shows the associated deflections for a 1.5-in. diameter epoxy-coated dowel bar, a 1.5-in. diameter GFRP dowel bar, and a medium elliptical steel dowel bar. The deflections are arranged starting with the largest values and going to the smallest values.

In Table 7.1, the significance of each deflection term relative to the others can easily be seen. The flexural deflection is approximately half of the next closest deflection term. This small deflection value indicates why almost no effect was seen on the modulus of dowel support and the concrete bearing stress. Another interesting item that can be seen above is that in the two round dowel bars, the shear deflection is greater than the slope deflection value. However, in the elliptical dowel bar, the slope deflection has a slightly larger value than the shear deflection. This trend clearly indicates that other deflections need to be considered as alternative dowel bar shapes are being investigated.

The following conclusions can be made about contraction joints with a 1/8-in. gap based on the research discussed previously.

- Friberg's addition of the bar width, b, in the Beta term causes the bearing stress value to be assumed constant across the entire bar width.
- Slope deflection value is similar to shear deflection for all the dowel bars used in this research.
- Slope deflection has a slightly larger effect on elliptical and GFRP dowel bars.

- Neglecting slope deflection caused the modulus of dowel support and the concrete bearing stress to be underestimated. While the overall effect on the modulus of dowel support and concrete bearing stress were not significant for the dowel bars used in this research, this effect may not be the case for dowel bars of all shapes, materials, and sizes.

- Neglecting slope deflection in previous research had no effect on the trends that were noted. However, the actual values may vary slightly from what was reported.

- Flexural deflection was shown to have an insignificant effect on the previously reported research values.

Table 7.1 – Total relative deflection, deflection at the face of the joint, shear deflection, slope deflection, and flexural deflection

	1.5"ϕ Epoxy-Coated	**1.5"ϕ GFRP**	**Medium Elliptical Steel**
Total Relative Deflection, Δ, in.	2.64 E-03	3.73 E-03	2.43 E-03
Deflection at the face of the joint, y_o, in.	1.26 E-03	1.45 E-03	1.16 E-03
Shear Deflection, δ, in.*	2.01 E-05	6.81 E-04	1.68 E-05
Slope Deflection, $z\left(\frac{dy_o}{dx}\right)$, in.*	1.01 E-04	1.44 E-04	9.64 E-05
Flexural Deflection, $\frac{Pz^3}{12EI}$, in.*	9.37 E-08	2.66 E-07	9.55 E-08

* Deflections cannot be measured this accurately but are shown for informational purposes

7.3 Recommendations

The following areas are recommended for further study:

- Investigate the appropriateness of the addition of the bar width in the Friberg deflection equations. The bar width assumes that the bearing stress is equally distributed across the bar width. This effect needs to be checked to verify if

accurate for round dowel bars, as well as alternatively shaped dowel bars. The investigation should also check the effect on other GFRP and steel dowel bars.

- The effect of joint width on flexural deflection should be studied further. As shown previously, flexural deflection is such a small amount of deflection for contraction joints. However, as the joint width increases the flexural deflection increases by a cubic. Therefore, a small change in joint width could significantly increase the flexural deflection.

- The effect of joint width on form factor should also be investigated further. With the small 1/8" joint width used in this research the form factor had little effect on the overall values of modulus of dowel support, deflection at the face of the joint and concrete bearing stress. However, if the joint width changes the form factors could potentially influence the values studied.

- Movement of the dowel bar can occur during the construction process. One possible outcome is that the dowel bar can become "sloped" across the pavement joint prior to the curing of the concrete. The effect of a dowel bar that is installed sloped across the pavement joint should also be studied. The effect that a sloped dowel bar has on the overall deflection and, more specifically, the slope deflection should be implemented.

REFERENCES

1. Federal Highway Administration. Highway Statistics 2000. *National Highway System Length – 2000; Miles by Functional System (Table HM-41).* Retrieved May 3, 2003, from http://www.fhwa.dot.gov/ohim/hs00/hm41.htm.

2. Federal Highway Administration. Highway Statistics 2000. *Federal-Aid Highway Length – 2000; Miles by Type of Surface (Table HM-31).* Retrieved May 3, 2003, from http://www.fhwa.dot.gov/ohim/hs00/hm31.htm.

3. Federal Highway Administration. Status of the Nation's Highways, Bridges, and Transit: 2002 Conditions and Performance Report to Congress. *Comparison of System Conditions Statistics with Those in the 1999 Report (Exhibit 3-1).* Retrieved May 3, 2003, from http://www.fhwa.dot.gov/policy/2002cpr/ch3.htm.

4. Iowa Department of Transportation. Standard Road Plans, RH Series Rigid Pavements and Associated Work. *Non-Reinforced Four-Lane 53 foot P.C. Concrete Pavement.* Retrieved May 4, 2003, from ftp://165.206.203.34/design/stdrdpln/english/erh47b.pdf.

5. Guinn, R. J. Assessment of Highway Pavement Slab Dowel Bar Research. *Masters Thesis*. Ames, IA, Iowa State University, 2002.

6. Timoshenko, S. and J.M. Lessels. *Applied Elasticity*. Westinghouse Technical Night School Press, East Pittsburgh, Pennsylvania, 1925.

7. Bradbury, R.D. Design of Joints in Concrete Pavements. *Proceedings, 12th Annual Meeting of the Highway Research Board*, pp. 105-141, Washington D.C., 1932.

8. Timoshenko, S. *Strength of Materials- Part II.* Robert E. Krieger Publishing Co., Inc, Huntington, NY, 1976.

9. Friberg, B.F. Design of Dowels in Transverse Joints of Concrete Pavements. *Transactions, American Society of Civil Engineers*. Vol. 105, No. 2081, 1940.

10. Albertson, M.D. Fibersomposite and Steel Pavement Dowels. *Masters Thesis*. Ames, IA, Iowa State University, 1992.

11. Porter, M.L., M. Alberston, B. Barnes, E. Lorenz, and K. Viswanath. Thermoset Composite Concrete Reinforcement. *Report HR-325 Submitted to Project Development Division of the Iowa Department of Transportation and Iowa Highway Research Board.* Ames, IA, May 1992.

12. Porter, M.L., D. Davis, R. Guinn, A. Lundy and J. Rohner. Investigation of Glass Fiber Composite Dowel Bars for Highway Pavement Slabs. *Report TR-408 Submitted to Project Development Division of the Iowa Department of Transportation and Iowa Highway Research Board.* Ames, IA, June 2001.

13. Serra-Conrads, L. Structural Analysis Considering Shear Deformations. *Masters Thesis.* Ames, IA, Iowa State University, 1962.

14. Young, W.C., *Roark's Formulas for Stress and Strain, Sixth Edition.* McGraw-Hill, Inc., New York, NY, 1989.

15. ACI Committee 325. Structural Design Considerations for Pavement Joints. *Journal of the American Concrete Institute*, Vol. 28, No. 1, July 1956, pp. 1-28.

16. Porter, M.L., R. Guinn, and A. Lundy. *Dowel Bar Optimization: Phases I and II, Final Report.* Submitted to American Highway Technology, Center for Transportion Research and Education, and the Center for Portland Cement Concrete Pavement Technology. Ames, IA, Iowa State Univeristy, 2001.

17. Walrath, D.E., and Adams, D.F., The Iosipescu Shear Test as Applied to Composite Materials. *Experimental Mechanics*, pg. 105-110, Brookfield Center, CT, March 1983.

18. American Association of State Highway and Transportation Officials (AASHTO). *AASHTO Guide for Design of Pavement Structures.* AASHTO, Washignton, D.C., 1993.

19. Rohner, J.G. Investigation of the Modulus of Dowel Support in Concrete Pavements. *Masters Thesis.* Ames, IA, Iowa State University, 1999.

20. Boris, T.A. Performance of Glass Fiber Reinforced Polymer Reinforcements in Simulated Concrete Environments. *Masters Thesis.* Ames, IA, Iowa State University, 1999.

21. Ugural, A.C., and Fenster, S.K., *Advanced Strength and Applied Elasticity, 3rd edition.* Prentice-Hall, Inc., Upper Saddle River, NJ, 1995.

22. Porter, M.L., B. Barnes, B. Hughes, and K. Viswanath. Non-Corrosive Tie Reinforcing and Dowel Bars for Highway Pavement Slabs. *Final Report HR-343 Submitted to Highway Division of the Iowa Department of Transportation and Iowa Highway Research Board.* Ames, IA, November 1993.

23. Porter, M.L., D. Davis, and J. Rohner. Investigation of Glass Fiber Composite Dowel Bars for Highway Pavement Slabs. *Progress Report TR-408 Submitted to Project Development Division of the Iowa Department of Transportation and Iowa Highway Research Board.* Ames, IA, January 1999.

ACKNOWLEDGEMENTS

The research described herein was conducted at the Iowa State University Structural Engineering Laboratories in the Department of Civil and Construction Engineering through the promising success of the Engineering Research Institute and sponsored by the Highway Division of the Iowa Department of Transportation (IDOT), the Center for Transportation Research and Education (CTRE), the Center for Portland Cement Concrete Pavement (PCC Center), and American Highway Technology (AHT). The author would like to thank the personnel at the IDOT and AHT who provided support through their experience and knowledge toward the project, namely, Mark Dunn (IDOT) and Steven L. Tritsch (AHT).

The author would especially like to thank Dr. Max Porter for allowing the opportunity to work on this research project. The author would also like to thank all of those involved for their efforts, but special thanks are given to Dr. Jim Cable who provided support through his expertise and knowledge toward the project and Dale Harrington, Director of the PCC Center, for his project administration leadership.

The author would also like to recognize and thank several firms for providing materials, services, and advice, including: Doug Gremel from Hughes Brothers, Inc. of Seward, Nebraska; James P. McCallion from RJD Industries, Inc. of Laguna Hills, California; and Technical Services, Inc. of Ames, Iowa.

The author would also like to acknowledge the support provided by Douglas L. Wood, Structural Engineering Laboratory Supervisor, for his expertise and assistance.